AD-A048 741 YALE UNIV NEW HAVEN CONN SYSTEMS AND INFORMATION SCIENCES F/G 20/1
FREQUENCY SPREADING IN FORWARD SURFACE SCATTERING.(U)
DEC 77 J G ZORNIG N00014-77-C-0237
UNCLASSIFIED S/IS-7710 NL

1 OF 1
AD
A048741

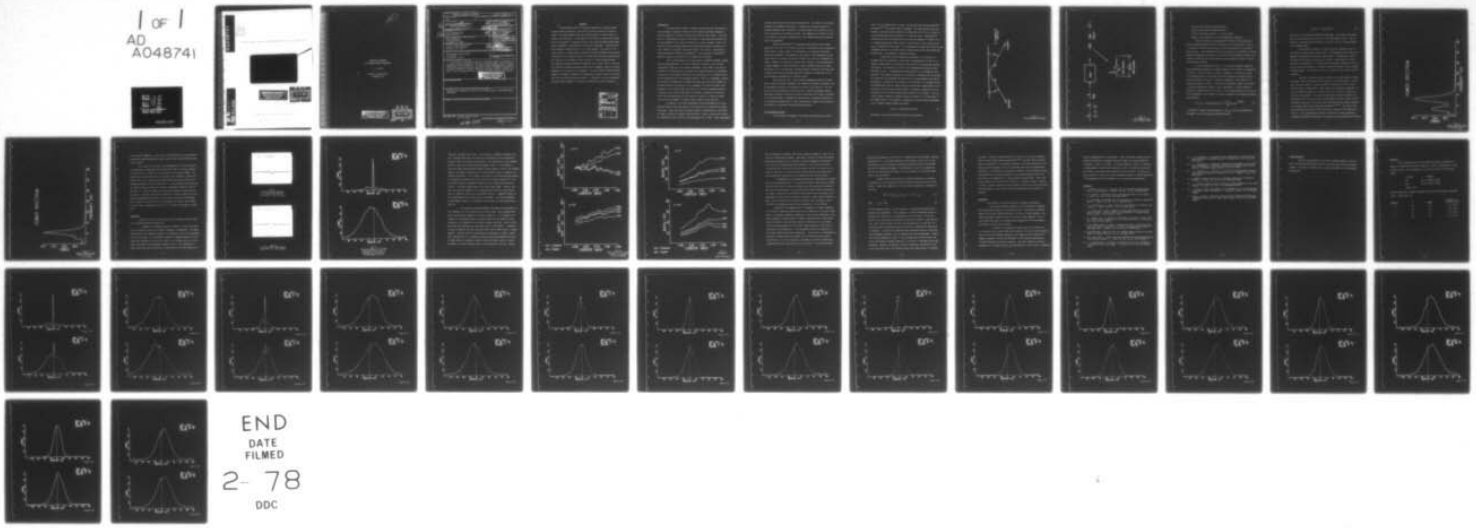

END
DATE
FILMED
2-78
DDC

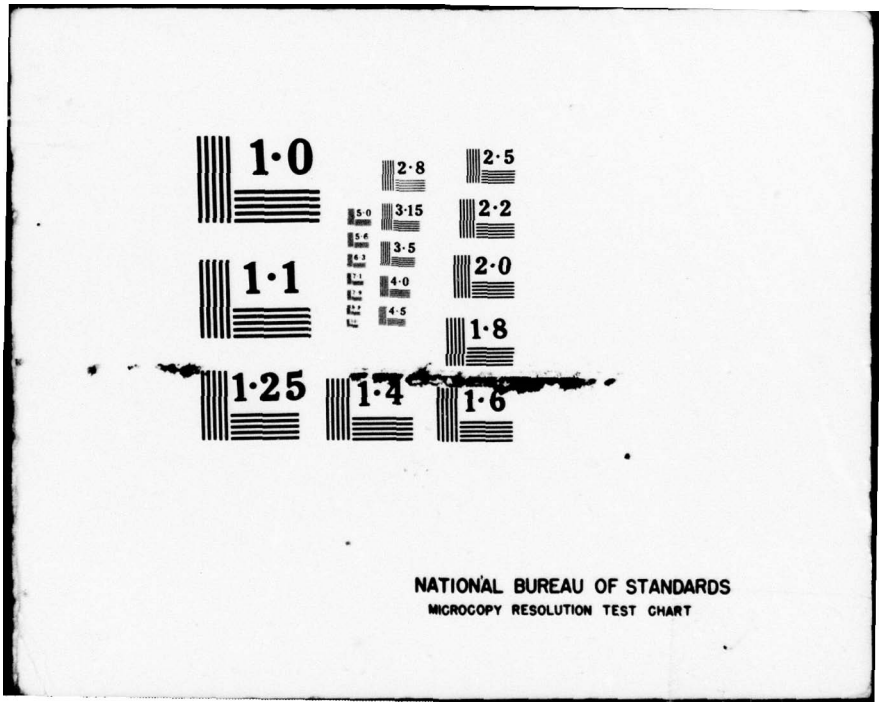
1·0
1·1
1·25
1·4
1·6
1·8
2·0
2·2
2·5
2·8
3·15
3·5
4·0
4·5
5·0
5·6
6·3
NATIONAL BUREAU OF STANDARDS
MICROCOPY RESOLUTION TEST CHART

# FREQUENCY SPREADING
# IN FORWARD SURFACE SCATTERING

J. G. Zornig

Technical Report #7710
December 1977

SECURITY CLASSIFICATION OF THIS PAGE (When Data Entered)

## REPORT DOCUMENTATION PAGE

READ INSTRUCTIONS BEFORE COMPLETING FORM

1. REPORT NUMBER: 7710
2. GOVT ACCESSION NO.:
3. RECIPIENT'S CATALOG NUMBER:

4. TITLE (and Subtitle): FREQUENCY SPREADING IN FORWARD SURFACE SCATTERING
5. TYPE OF REPORT & PERIOD COVERED: Technical Report,
6. PERFORMING ORG. REPORT NUMBER: S/IS-7710

7. AUTHOR(s): John G. Zornig
8. CONTRACT OR GRANT NUMBER(s): N00014-77-C-0237, N00014-75-C-1014

9. PERFORMING ORGANIZATION NAME AND ADDRESS:
YALE UNIVERSITY
15 Prospect Street
New Haven, CT 06520

10. PROGRAM ELEMENT, PROJECT, TASK AREA & WORK UNIT NUMBERS:
NR 083-322/12/30/76 (480D)
NRL Req. N00173-75-RQ-6410/
3-14-75

11. CONTROLLING OFFICE NAME AND ADDRESS:
Office of Naval Research
Arlington, VA 22217

12. REPORT DATE: Dec [redacted] 77
13. NUMBER OF PAGES: 42p.

14. MONITORING AGENCY NAME & ADDRESS (if different from Controlling Office):
ONR Resident Representative
715 Broadway
New York, NY 10003

15. SECURITY CLASS. (of this report): U
15a. DECLASSIFICATION/DOWNGRADING SCHEDULE:

16. DISTRIBUTION STATEMENT (of this Report)

The content of this report does not necessarily reflect the position or the policy of the Department of the Navy or the Government, and no official endorsement should be inferred. The United States Government has at least a royalty-free, non-exclusive and irrevocable license throughout the world for Government purposes to publish, translate, reproduce, deliver, perform, dispose of, and to authorize others so to do, all or any portion of this work.

DISTRIBUTION STATEMENT A
[redacted] Approved for public release; Distribution Unlimited

18. SUPPLEMENTARY NOTES

19. KEY WORDS (Continue on reverse side if necessary and identify by block number)
Communication, Underwater Acoustics, Scattering, Doppler, Spreading, Model, Experiment

20. ABSTRACT (Continue on reverse side if necessary and identify by block number)

DD FORM 1 JAN 73 1473 EDITION OF 1 NOV 65 IS OBSOLETE
S/N 0102-014-6601

SECURITY CLASSIFICATION OF THIS PAGE (When Data Entered)

410 215

## ABSTRACT

An experimental study of frequency spreading in acoustic signals forward scattered from model tank wind driven water surfaces has been performed. The study employed wide band probing signals to doubly sample the surface scatter process. A high degree of precision and demonstrated repeatability was produced. Parameters varied in the study included grazing angle, surface roughness, wind direction, and acoustic wavelength. Rayleigh roughness parameters varying from 0.7 to 12. were studied. The results of the study consist of a large number of measured frequency spreading functions and an analysis of the frequency shift of the mean scattered power and RMS spread as a function of wavelength for each condition of wind and grazing angle. This analysis indicates qualitative agreement with current theory in the general form of the spread spectrum at high and low roughness, and in the linear dependence of the mean shift on frequency. The data showed a marked sideband asymmetry in symmetric geometric configurations, however, which is not consistent with any published analytical model. In addition, at short wavelengths, frequency spread seemed not to increase linearly with carrier frequency.

Introduction:

In recent years a number of studies, both theoretical and empirical, have attempted to explain the nature of the frequency spreading undergone by acoustic signals as a result of interaction with the ocean surface. The problem is of considerable interest in the design of long range sonar systems and in the estimation of sea surface statistics by acoustic methods. Recent theoretical work has included approximate integral formulations by Roderick and Cron[1], Parkins[2], Williams[3], Scharf and Swarts[4], and Tuteur[5], a perturbation theory based model of Harper and LaBianca[6,7], and an analysis by Middleton[8] based on a model of the surface as an ensemble of scatterers.

Each of these models is of course based on somewhat different assumptions and approximations. It is not surprising, therefore, that the predictions made by them are not in complete agreement. There seems to be wide acceptance of the assertion that in general the temporal spectrum of waveheights in the area of the surface involved in the scattering will be a primary factor in the determination of the spreading function. There is no agreement, however, on the nature and magnitude of asymmetry between upper and lower sidebands to be expected and on the question of the appearance of second and higher order harmonics of the surface height spectrum in the frequency spreading function. In addition, the relative importance for frequency spreading of diffraction effects and the sensitivity of the function to implicit or explicit assumptions about the asymmetry of surface slopes remains an open question.

Fortunately, two recent experimental studies performed in the ocean have been able to shed some light on these questions for long and short range situations. Brown and Frisk[9] performed a number of measurements in the Pacific at ranges of 488 and 152 meters (1600 and 500 ft.) and at relatively low acoustic frequencies (100 to 500 Hz.) and waveheights (29 cm. RMS). These measurements

represent single bounce weak scattering situations. The results of these measurements were somewhat inconclusive. Evidence was presented, however, of sideband asymmetry and the presence of possible higher order functions of the surface spectrum in the acoustic spectra. The asymmetry was confined to relative heights of individual components and total sideband power was in general found to be symmetric.

Shooter and Mitchell[10] in subsequent measurements at much longer ranges (93 to 370 km.) in the deep ocean and at substantially lower frequencies (92 and 137 Hz.) gave an idea of the spreading to be expected in multiple bounce RSR situations. Unfortunately, this aspect of the experimental situation restricts the extent to which the results can be used as a benchmark for theory. However, the presence of higher order structure in the sidebands and a marked asymmetry in power favoring the higher sideband observed at higher sea states (2.1 m. sea and swell, confused surface) reinforces the notion that a simple function of the surface spectrum is probably not sufficient to explain frequency spreading due to surface scatter.

The situation, then, is that several mathematical models are available to predict frequency spreading, each exhibiting different properties, and no experimental evidence is available with which to sort them out. The purpose of the work presented in this paper was to produce experimental data of sufficient precision and variety to permit a more decisive relative evaluation of the current models. Although this work does not unilaterally support any of the models mentioned above, it does clearly show a number of the controversial effects in relatively clearly defined situations.

## The Experimental Method:

The experiments discussed in this paper were conducted in a model

tank 7.3 m. in diameter and 1 m. deep. The facility used has been described previously[11,12] and remains largely unchanged. The rough surfaces were produced by a fan driven wind tunnel with an effective fetch of 3.4 m. upwind of the scattering area and wind speeds of 5.4 and 8.3 m./sec. Reflections of surface waves from the downwind end of the tank are damped by a "beach" so as to suppress free gravity waves (swell). This was done so as to study the effects of wind driven waves alone. All measurements were made with projector and hydrophone directed at the mean surface specular point and at equal depth and grazing angle. The geometry is defined in Figure 1.

A technique of doubly sampling the response of the surface to a broadband pulse was employed in this series of measurements as a way of acquiring a large amount of precise data efficiently while suppressing spurious reflections. The procedure is based on the preemphasized pulsing technique described in [11]. A preemphasized probing signal s(t) is designed and synthesized. This signal is applied to the projector, interacts with the surface, is received by the hydrophone and digitized at the same sampling rate used to synthesize it. Because of the linearity of the process, it is assumed and has been demonstrated that the signal waveform received after digitization is the convolution of the original probing signal, the impulse responses of the two transducers, and the time varying impulse response of the surface. Since the surface impulse response is slowly varying with respect to the time scale of the signal itself, it is possible to represent this process after transformation to signal frequency domain as follows:

$$R(\omega_n,t) = S(\omega_n)P_0(\omega)H(\omega,t)P_1(\omega) \qquad (1)$$

where $S(\omega_n)$ is the probing signal applied to the projector

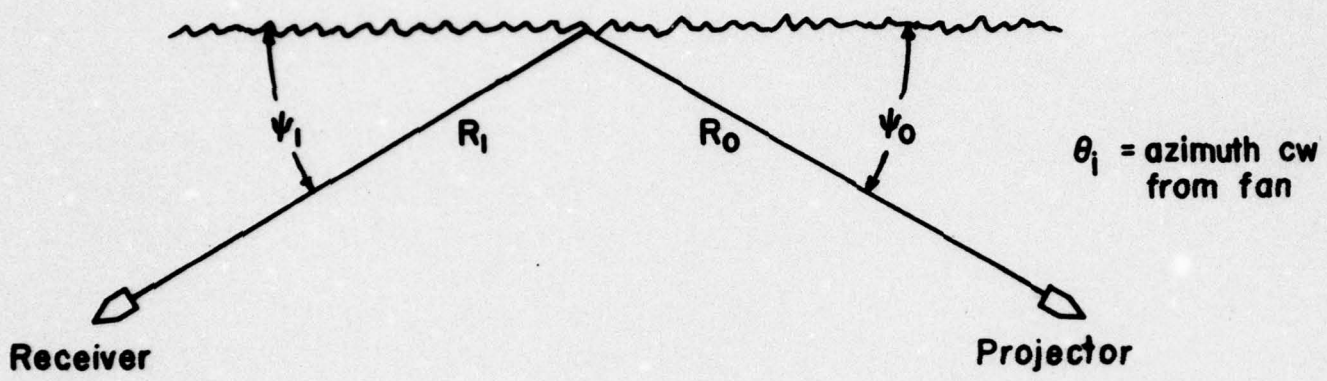


Fig. 1:
The experimental geometry

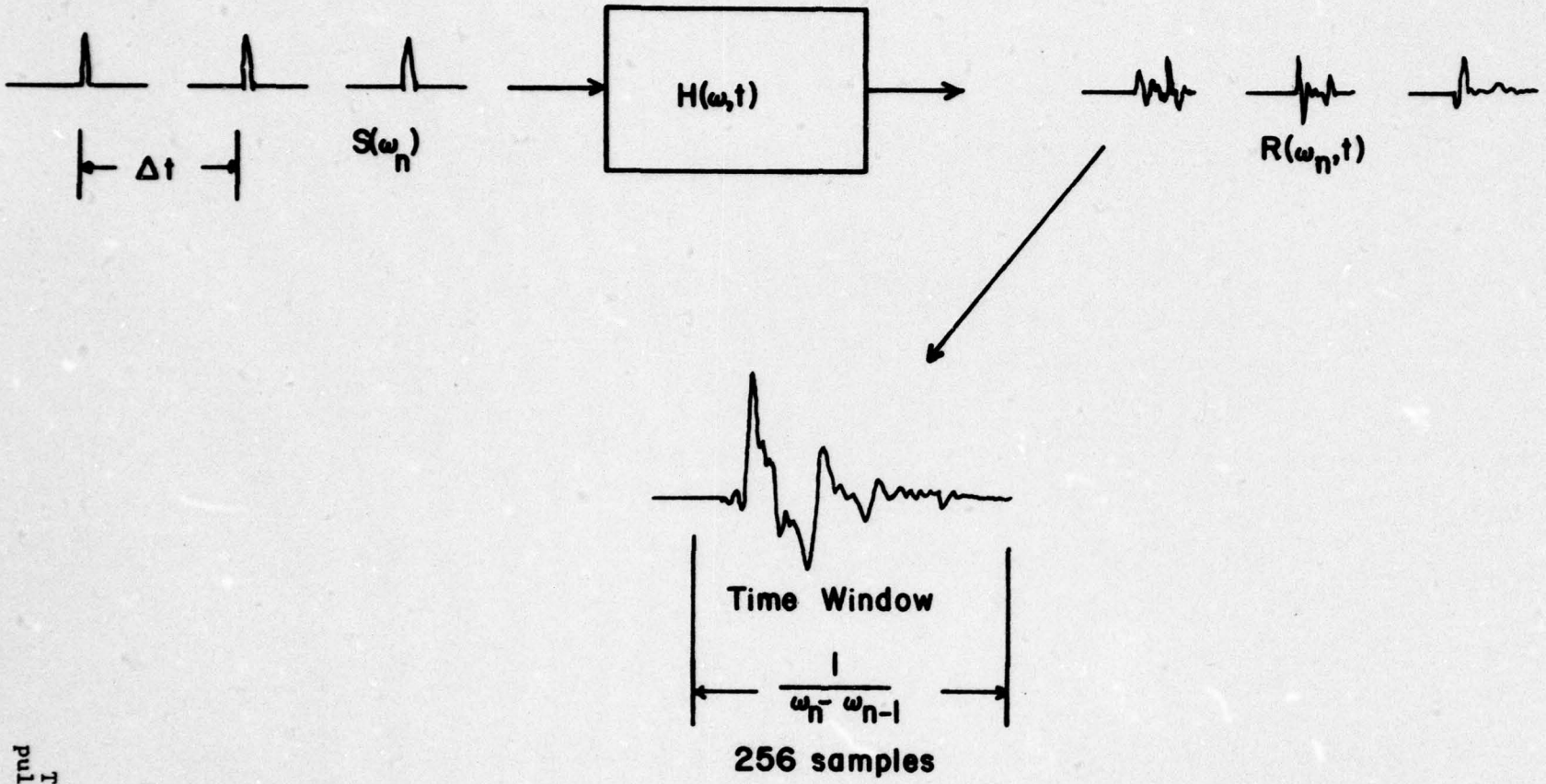


Fig. 2:
The timing of the
pulse probing system

$P_0(\omega)$ is the projector transfer function

$P_1(\omega)$ is the receiver transfer function

$H(\omega,t)$ is the time varying T. F. of the surface

$R(\omega_n,t)$ is the signal out of the hydrophone and amplifiers

The data collection instrumentation[13] removed a fixed time delay from the received signals which is reflected in the notation here in the use of the same t in both $H(\omega,t)$ and $R(\omega_n,t)$ and the suppression of time dependence in $S(\omega_n)$. The representation of $S(\omega_n)$ and $R(\omega_n,t)$ as defined on a finite domain of frequencies is based on the fact that both waveforms are wholly contained in relatively short time windows and are analysed in terms of the discrete Fourier transform.

In this representation, $H(\omega,t)$ is a stationary ergodic random process expressing the amplitude and phase response of the surface to frequencies $\omega$ at time t. Care was taken, of course, to sample in t at rates in excess of the Nyquist rate of the process; the actual sampling rate used varied between 50 and 300 per second. In practice, sampling in t was limited to 64 contiguous samples in a burst. This limit was imposed by memory availability in the data acquisition computer, and is equivalent to CW pulse lengths of from 850 to 20,000 cycles of the carrier. The recorded samples of $H(\omega,t)$ were then transformed on the variable t to give an ensemble of instantaneous spreading functions.

$$F(\omega_n,\nu_k) = (S(\omega_n)P_0(\omega_n)P_1(\omega_n))^{-1}(\Delta t \sum_{m=0}^{N-1} R(\omega_n,t_m)e^{-j\nu_k m\Delta t}) \qquad (2)$$

An ensemble of roughly 200 measurements of $F(\omega_n,\nu_k)$ were then windowed and averaged to give the frequency spreading function,

$$\Phi(\omega_n, \nu_k) = \langle F(\omega_n, \nu_k) * W(\nu_k) \rangle \qquad (3)$$

where $W(\nu_k)$ is the frequency domain Hanning window. The design of the signal $S(\omega_n)$ was such that the first term in (2) was approximately unity. This resulted in a uniformly precise estimate of $\Phi(\omega_n, \nu_k)$ over the frequency domain of the probing signal.

This procedure turned out to have substantial advantages over the alternative of using single long CW pulses. The advantages are the near total immunity from multipath interference made possible by time gating of broad band pulses, and parallel acquisition of data at a large number of carrier frequencies simultaneously. The principal disadvantage at present is the relatively restricted resolution in Doppler frequency obtainable with the present available memory. This turned out not to be a problem in this series of measurements.

Data were collected using this scheme for two wind speeds, two grazing angles, and two orientations with respect to the wind direction. In each case, over 100 values of $\omega_n$ were available from the data of which 4 values were selected for presentation. These results are displayed in Appendix A as plots of Doppler frequency vs. relative power for a variety of values of $\omega_n$, wind speed and geometry. The water surface temporal spectra, measured by a capacitance probe, for each of the two wind speeds are shown in Figs. 3 and 4. The general properties of the short fetch wind driven water surfaces produced in the model tank have been discussed previously[11,12,14]. The spectra have been included here because of their relevance to several of the theories referred to. These measurements represent conditions of strong scattering, crosswind and downwind orientation, and long and short wavelengths with respect

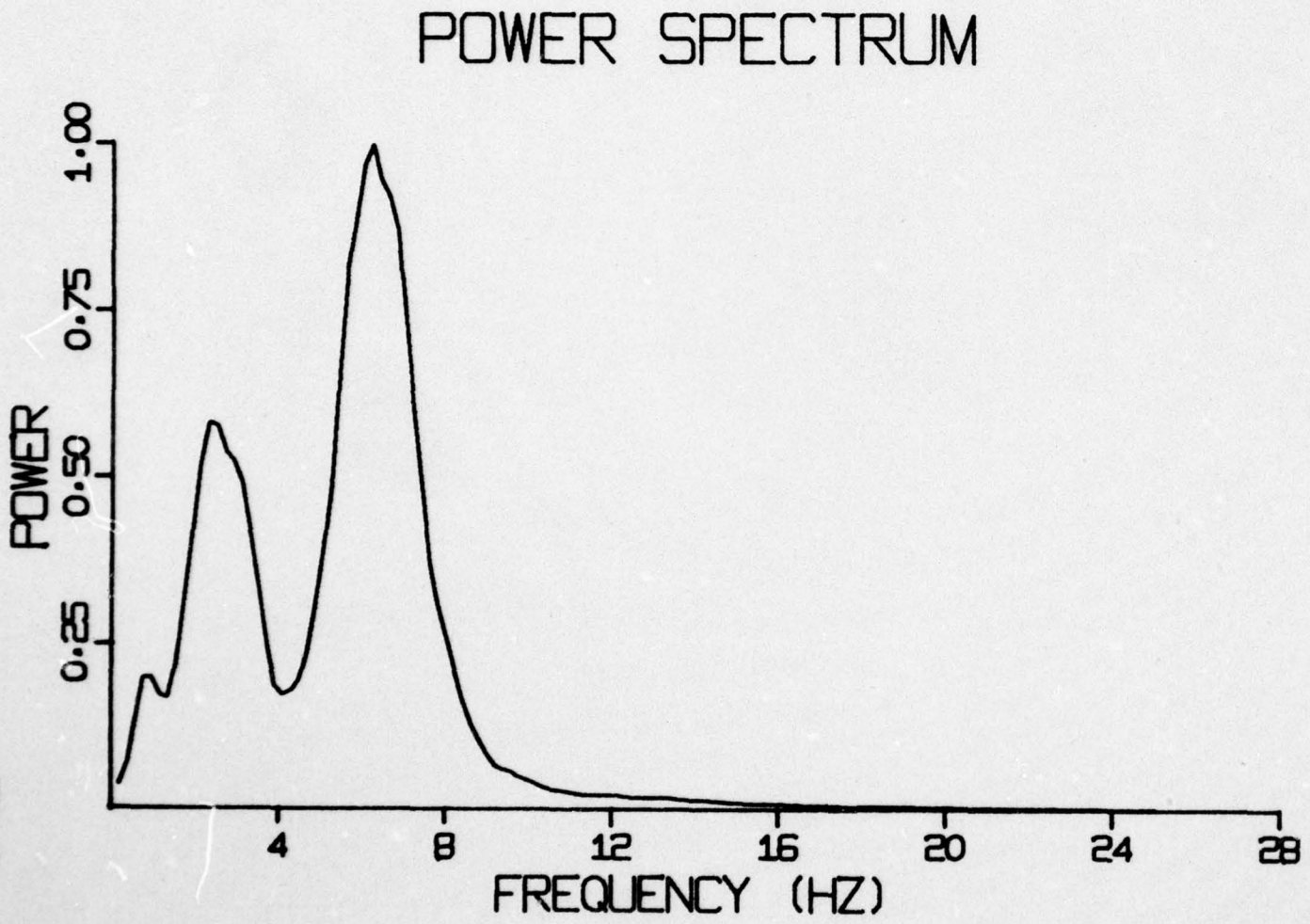


Fig. 3:
Surface temporal power spectrum for Wind 2, $\sigma$ = 1.1 mm.

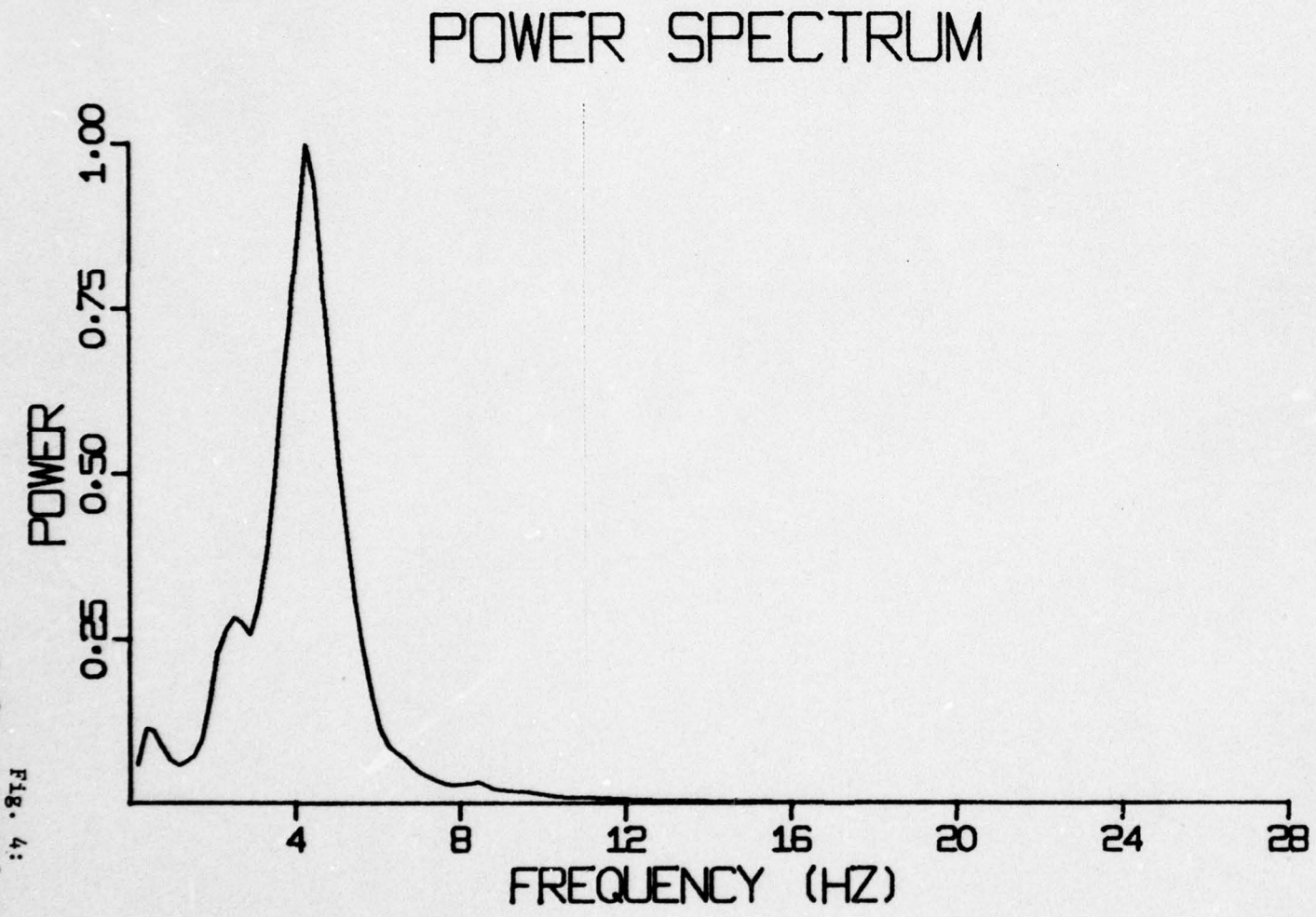


Fig. 4:
Surface temporal power spectrum for Wind 4, $\sigma$ = 2.6 mm.

to the surface roughness. In all cases, the beam patterns of the projector/receiver pair were substantially larger than the first several Fresnel zones on the surface.

As a check on the linearity and repeatability of the data acquisition apparatus, an experiment was performed which was in all ways identical to that of Fig. A-1, except for a modification of the probing signal. The signal used to obtain the spectra in Appendix A was designed to present the receiver with a flat spectrum pulse having essentially equal energy at all frequencies between 0.2 and 1.2 MHz (Fig. 5). The pulse used in the test run was similar except for deletion of spectral components between 0.6 and 0.9 mHz (Fig. 6). These two signals obviously differ greatly in their time domain forms. Therefore, they could be expected to provide a good test of the linearity assumptions upon which the data analysis procedure used depends. Fig. 7 shows the results of the test measurement for 256 kHz. and 1.06 MHz. As can be seen by comparison with Fig. A-1, the degree of agreement is quite good.

Discussion:

Inspection of the results presented in the previous section reveal the following qualitative observations:

1. Asymmetry of frequency spread is observed to be the rule rather than the exception, even in the symmetric geometric configuration. The amount and direction of the asymmetry appears to be dependent on all of the parameters varied in the study. At low Rayleigh parameters, sidebands appear to have unequal power although the locations of peaks in the sideband spectra are coincident with peaks in the waveheight temporal spectra. This phenomenon is wholly consistent with the notion of a system function as used by Harper and

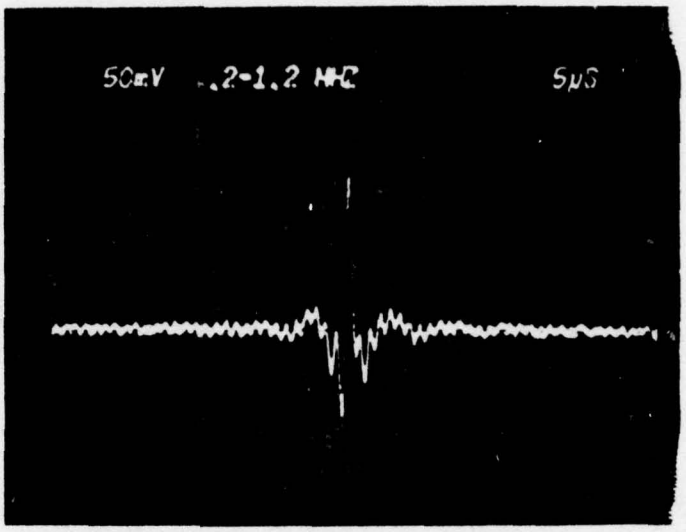


Fig. 5:
The probing pulse observed
at the receiver with a
flat surface. (0.2-1.2 MHz.)

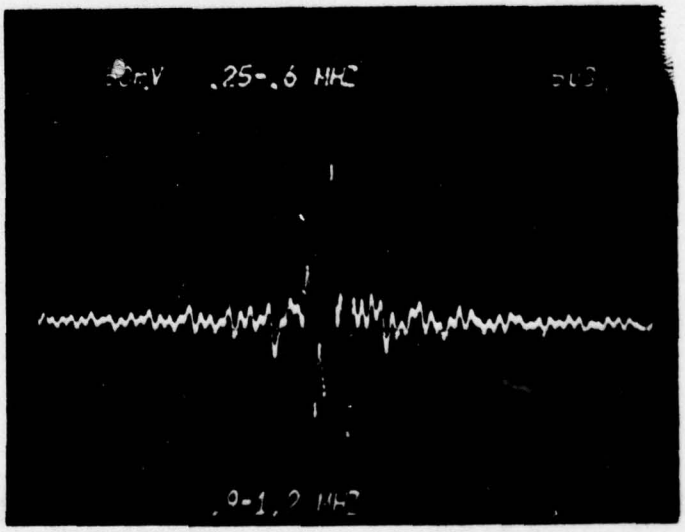


Fig. 6:
A special split band probing
pulse (0.25-.6, .9-1.2 MHz.)

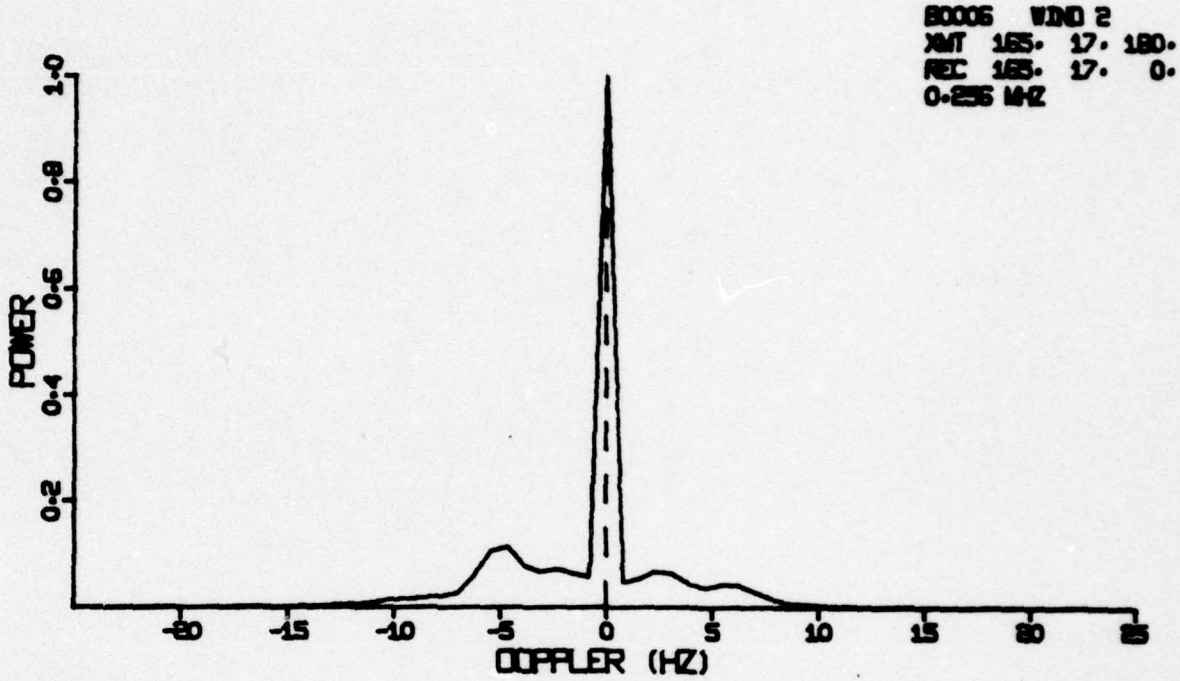


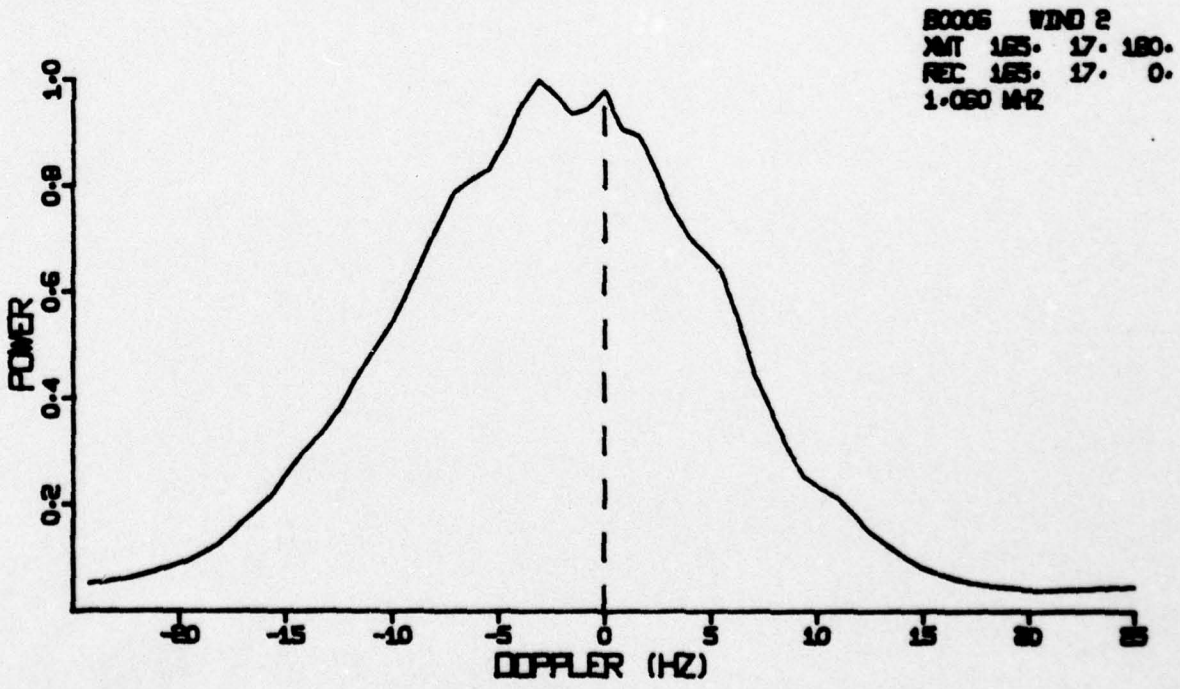


Fig. 7:
Frequency spread for the same conditions as Fig. A-1a, d measured with the special probing signal (Fig. 6)

LaBianca[6], Williams[3], and others. Its presence in a symmetric geometry, however, indicates that there are significant inadequacies in the formulations presently used to calculate these functions. The transition to high roughness appears to take place between Rayleigh numbers 1 and 2. In this domain, a relatively smooth approximately Gaussian spectrum appears to add to the weighted image of the surface spectrum until at values greater than 2 it dominates the frequency spreading. In this regime, the nature of the spread spectrum appears to be generally consistent with the prediction of Scharf and Swarts[4] in that the spread spectrum is generally Gaussian and with a mean shifted from the carrier by an amount proportional to the carrier wave number. However, this model also predicts symmetry in the configurations used here, and therefore does not completely account for the observed spectra. A suggested reason for this disagreement will be given later in this paper. The linear dependence on wave number, however, is consistent with the data, at least qualitatively (Fig. 8).

2. The frequency spreading bandwidth increases with increasing carrier frequency, but not linearly and not without limit. RMS spreading bandwidth versus carrier frequency is plotted in Figure 9. In the regime of low roughness, the bandwidth seems to increase slowly from an asymptotic value equivalent to the bandwidth of the surface temporal spectrum. This is hardly surprising and consistent with the models valid in that domain. In addition, the data of Roderick and Cron, Brown and Frisk, and Williams reflect a similar behavior. Roderick and Cron have proposed an explanation in terms of higher order sidebands due to a simultaneous phase and amplitude modulation process. At higher values of roughness, however, Scharf and Swarts predict a linear dependence on carrier frequency which is not supported by the data. Indeed,

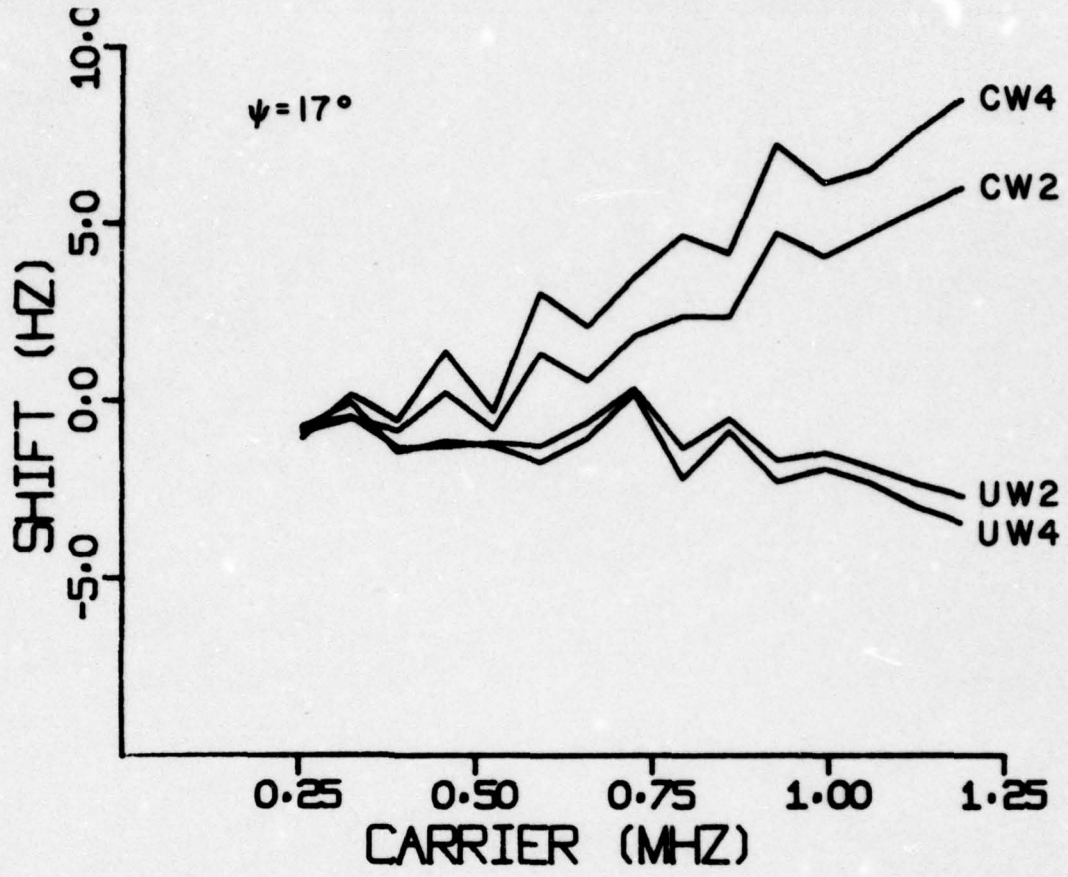


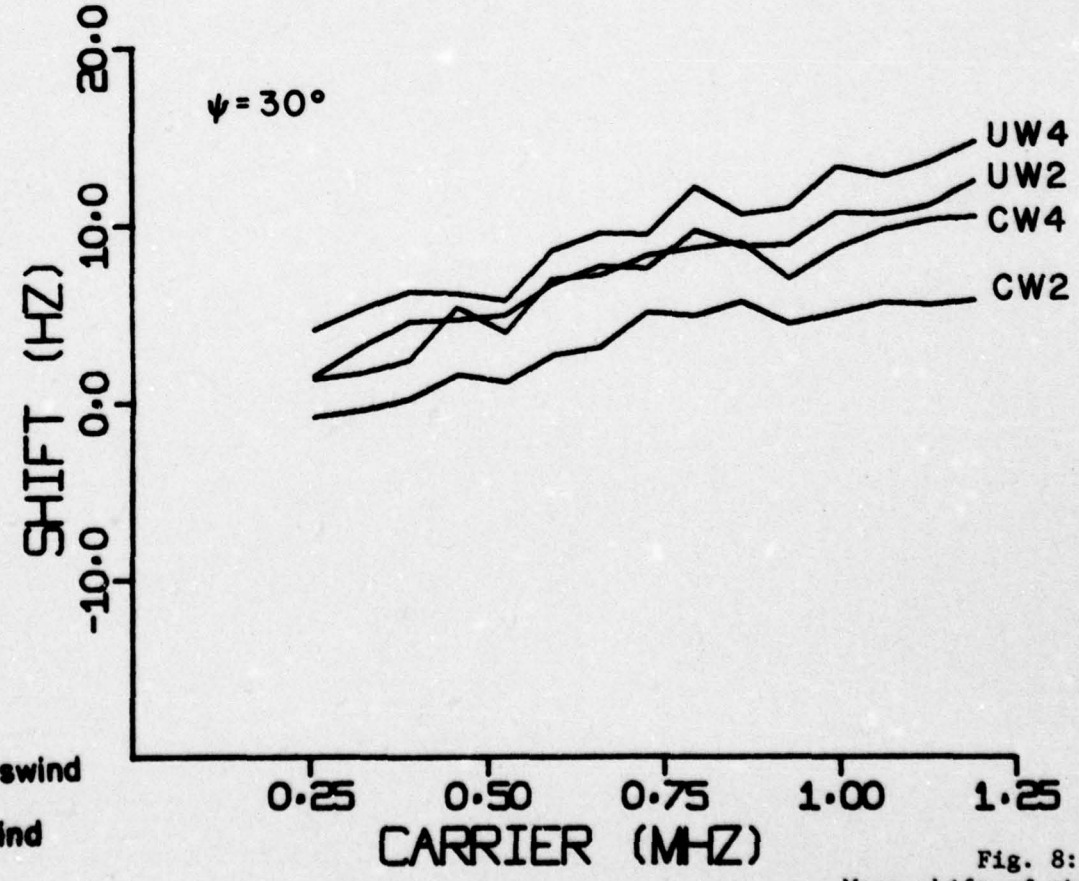


CW = Crosswind

UW = Upwind

Fig. 8:
Mean shift of the spread spectra vs. incident carrier frequency

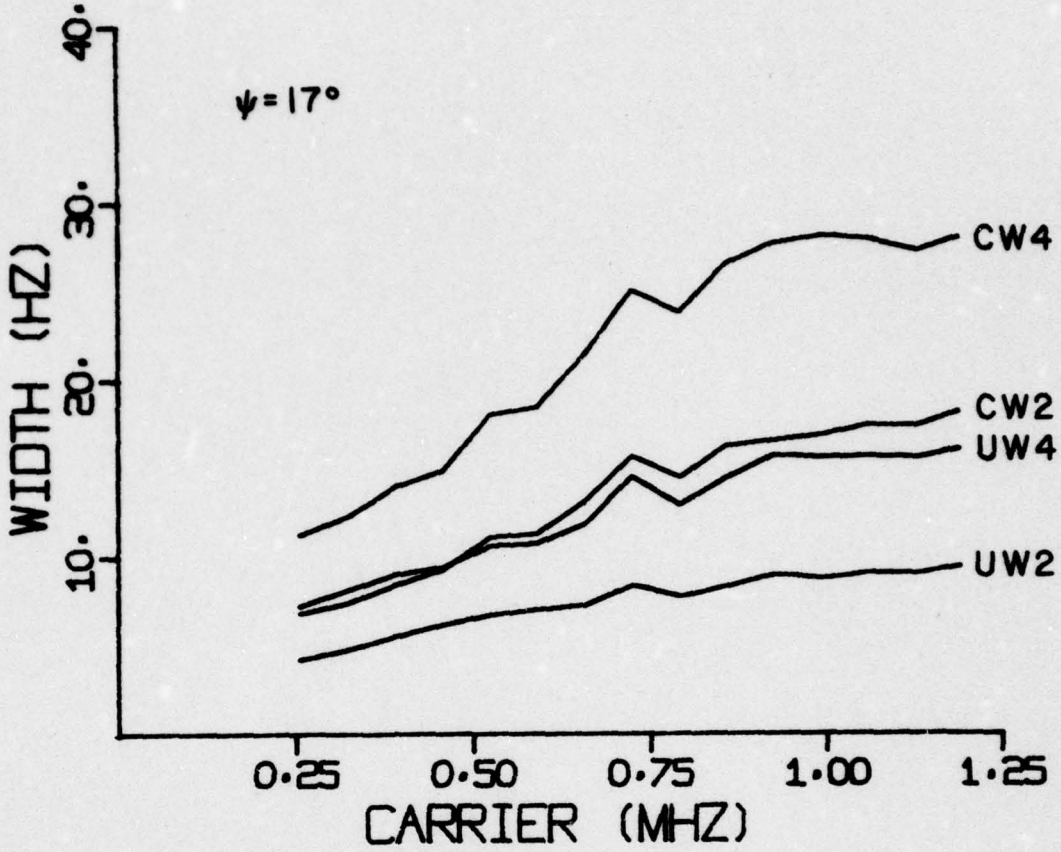


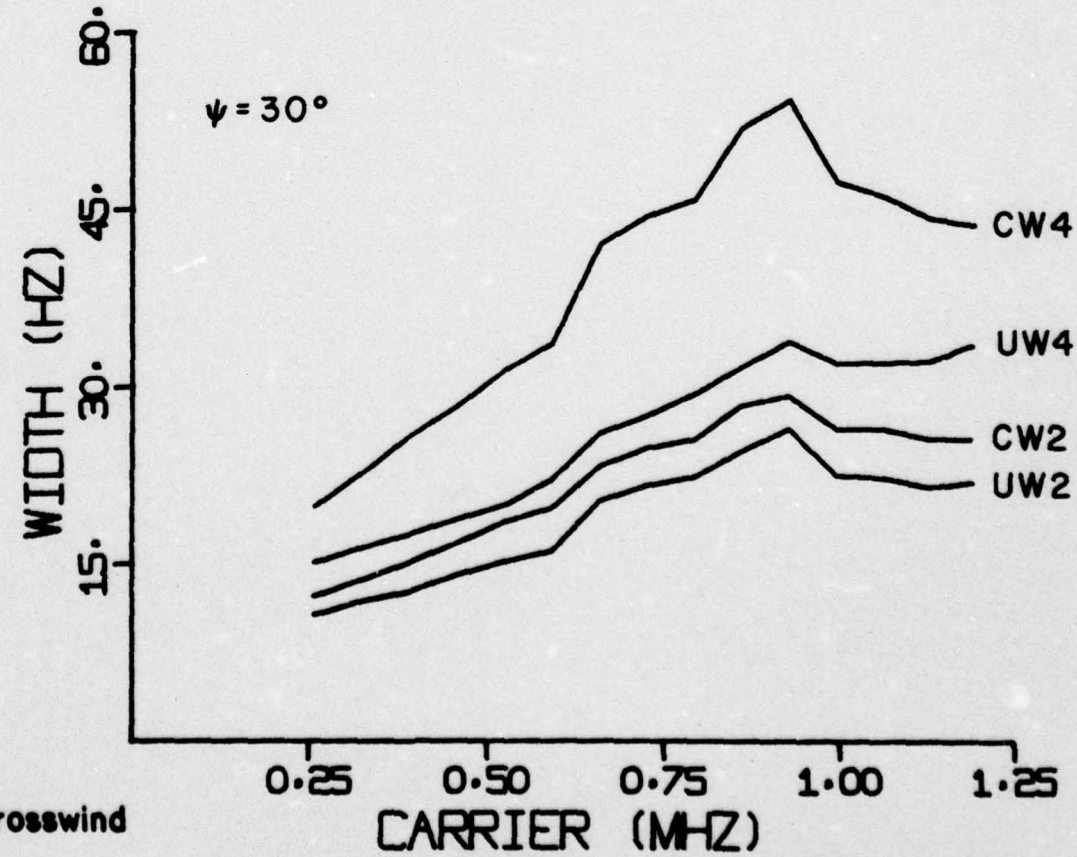


CW = Crosswind

UW = Upwind

Fig. 9:
RMS spread
vs.
carrier frequency

rate of increase of bandwidth with carrier frequency appears to taper off to zero and in some cases decreases. Apparently, the point at which the spreading stops increasing is not a function of surface roughness or wind direction, but only of grazing angle and wavelength. This has led the author to speculate that the cause of the levelling off may have to do with the decrease in the size of the first several Fresnel zones on the surface which are the principal contributors to the signal received from the surface.

3. Spreading in the crosswind orientation is substantially stronger than in the upwind direction. To a qualitative extent, this effect is consistent with the results of Scharf and Swarts that the spread can be predicted from the second derivatives of the surface space-time correlation function at the origin. Quantitative verification would require both an extensive set of measurements of the surface correlation functions at small lags and displacements, and a resolution of the symmetric geometry issue referred to above. The author is considering some practical approaches to both problems.

Middleton[8] has suggested that the inadequacy of current treatments of the Doppler spreading process stems from the tendency of the various treatments to incorporate incomplete treatments of the two basic mechanisms of frequency spreading. Doppler spread in signals reradiated from a rough moving surface arises both from individual physical interactions of the incident field with moving elements of the surface (phase modulation), and from the interference of contributions to the reradiated field due to variations in path length (amplitude and phase modulation). Surely these two mechanisms are intimately coupled through the dynamics of the wind driven water surface. Nevertheless, in all of the analytical treatments cited above, simplifying assumptions have been made which have the net effect of either inaccurately

modeling one mechanism or the other, or of neglecting the hydrodynamic coupling between the two. In the data presented in this paper, as well as, to a limited extent, in the ocean data, a substantial difference can be seen between high and low roughness spreading. This difference is not only in magnitude but also in form and may well have to do with a change in the relative importance of the two effects.

Another obvious and universally recognized weakness of the analytical models is in the relatively simple expressions usually used for the sea surface. Harper and LaBianca[7] use a fairly typical expansion in sinusoids of the form:

$$Z(\vec{\rho},t) = \frac{1}{\sigma} \sum_i \sum_j h_{ij} \cos(\Gamma_{ij} \cdot \vec{\rho} - \Omega_j t + \gamma_{ij}) \tag{4}$$

where $$|\Gamma_{ij}| = \Omega_j^2 g \tag{5}$$

and the component phases, $\gamma_{ij}$, are assumed to be uniformly distributed and statistically independent. This assumption of uniform independent phases is probably not realistic but is mathematically very convenient. Scharf and Swarts[4] use an equivalent representation expressed in terms of a spectral density. They correctly point out that this representation is valid only for a restricted class of Gaussian surfaces which are not significantly wind driven or turbulent. In view of the relatively well understood nature of scattering from sinusoidal interfaces, such an expansion has obvious advantages. Indeed, for a surface dominated by swell, or for a mechanically excited surface such as the one studied by Roderick and Cron[1], this form is a reasonably good representation. However, for surfaces in which a substantial contribution is due to the local wind (sea), the sinusoidal model with random phases is certainly

inaccurate. The most convincing evidence of this is to be found in measurements of water surface slope distributions[14,16,17] and wind direction dependence of backscatter[15]. The surfaces produced in the model tank used in this study have been designed to have a very minimal swell and are predominantly wind driven. It should not be surprising, therefore, that the Doppler spreading observed is not entirely predicted by the analytical models which have been based on an assumption of a simple surface representation. Actual wind driven surfaces are very difficult to model in a realistic fashion. However, in order to produce a generally useful predictive theory for ocean scattering, some improvements in the present surface representations will probably be required.

Conclusion:

The results of this study indicate two general conclusions:

1. The current theories proposed for the prediction of frequency from rough water surfaces do to some extent work. They predict a modified image of the surface temporal spectrum in the case of small roughness, and a shifted Gaussian of greater width in the case of large roughness. Both of these predictions seem to be qualitatively consistent with the experimental measurements on wind driven surfaces.

2. In general, the quantitative predictions of the theories are not accurate for the case of wind driven surfaces. The most obvious disagreements are that the observed spreading is not symmetric under conditions of symmetric geometry, and that the bandwidth of the scattered sound does not increase linearly with acoustic frequency. The exact reasons for this disagreement are at present obscure, but seem likely to be the result of incomplete

surface representations in the analyses. These conclusions indicate that the theoretical models are in general correctly formed, but require additional refinement in order to be useful. The author intends to direct his attention to measurements on surfaces with substantial swell, off-specular scattering, and studies of the second order statistics of the surfaces. In this way, it may be possible to arrive at a useful compromise between the limited generality of experimentation and the necessary evils of analytical approximation.

References:


1. W. Roderick and B. Cron, "Frequency Spectra of Forward Scattered Sound from the Ocean Surface," J. Acoust. Soc. Am., 48, pp. 759-766 (1970).

2. B. E. Perkins, "Scattering from the Time Varying Surface of the Ocean," J. Acoust. Soc. Am., 42, pp. 1262-1267 (1967).

3. R. G. Williams, "Estimating ocean wind wave spectra by means of underwater sound," J. Acoust. Soc. Am., 53, pp. 910-920 (1973).

4. L. L. Scharf and R. L. Swarts, "Acoustic scattering from a stochastic sea surface," J. Acoust. Soc. Am., 55, pp. 247-253 (1974).

5. F. B. Tuteur and H. Tung, "Asymmetric Doppler Amplitudes in the Surface Scatter Channel," Technical Report CS-7, Department of Engineering and Applied Science, Yale University (1976).

6. E. Y. Harper and F. M. LaBianca, "Scattering of sound from a point source by a rough surface progressing over an isovelocity ocean," J. Acoust. Soc. Am., 58, pp. 349-364 (1975).

7. F. M. LaBianca and E. Y. Harper, "Sideband structure of sound from a harmonic point source scattered by a rough surface moving over an upward refracting ocean," J. Acoust. Soc. Am., 61, pp. 378-389 (1977).

8. David Middleton, "Doppler effects for randomly moving scatterers and platforms," J. Acoust. Soc. Am., 61, pp. 1231-1250 (1977).

9. M. V. Brown and G. V. Frisk, "Frequency smearing of sound forward-scattered from the ocean surface," J. Acoust. Soc. Am., 55, pp. 744-749 (1974).

10. J. A. Shooter and S. K. Mitchell, "Observations of acoustic sidebands in cw tones received at long ranges," J. Acoust. Soc. Am., 60, pp. 839-842 (1976).

11. J. G. Zornig and J. F. McDonald, "Direct measurement of surface-scatter channel coherence by impulse probing," J. Acoust. Soc. Am., 55, pp. 1205-1211 (1974).

12. J. G. Zornig and J. F. McDonald, "Experimental measurement of the second-order interfrequency correlation function of the random surface scatter channel," IEEE Trans. Comm., COM-23, pp. 341-347 (1975).

13. J. G. Zornig and J. F. McDonald, "A High Speed Microprogrammed System for Generation and Acquisition of Signals," Rev. Sci. Instrum., 44, pp. 1217-1222 (1973).

14. H. Medwin, "Specular Scattering of Underwater Sound from a Wind-Driven Surface," J. Acoust. Soc. Am., 41, pp. 1485-1495 (1966).

15. J. G. Zornig, "Bistatic surface scattering strength measured at short wavelengths," J. Acoust. Soc. Am. (to be published in 1978).

16. C. Cox and W. Munk, "Measurement of the roughness of the sea surface from photographs of the Sun's glitter," J. Optical Soc. Amer., 44, pp. 838-850 (1954).

17. Allen H. Schooley, "Probability Distributions of Water-Wave Slopes under Conditions of Short Fetch," Trans. Amer. Geophys. Union, 39, pp. 405-408 (1958).

Acknowledgements:

This work was supported by the Office of Naval Research, Code 480, and by the Undersea Surveillance Division, Code 320, Naval Electronic Systems Command. The author is indebted to Ms. Jacqueline Snyder for the waveheight measurements.

Appendix A:

The following plots are of the measured frequency spreading for a variety of conditions and carrier frequencies. Each is identified by an identification block. The information in the block is given in the following format:

| Run No. | Wind No. |
|---|---|
| XMT | $R_0$(cm) $\psi_0$(deg) $\theta_0$(deg) |
| REC | $R_1$(cm) $\psi_1$(deg) $\theta_1$(deg) |
| Carrier Freq. | |

Surface roughness is commonly expressed as either RMS waveheight or Rayleigh delay. These values are:

| Wind No. | $\psi$ | $\sigma$(mm.) | $\frac{4\pi\sigma \sin \psi}{c}$ (sec) |
|---|---|---|---|
| 2 | 17° | 1.13 | $2.8 \times 10^{-6}$ |
| 2 | 30° | 1.13 | $4.8 \times 10^{-6}$ |
| 4 | 17° | 2.6 | $6.5 \times 10^{-6}$ |
| 4 | 30° | 2.6 | $11.1 \times 10^{-6}$ |

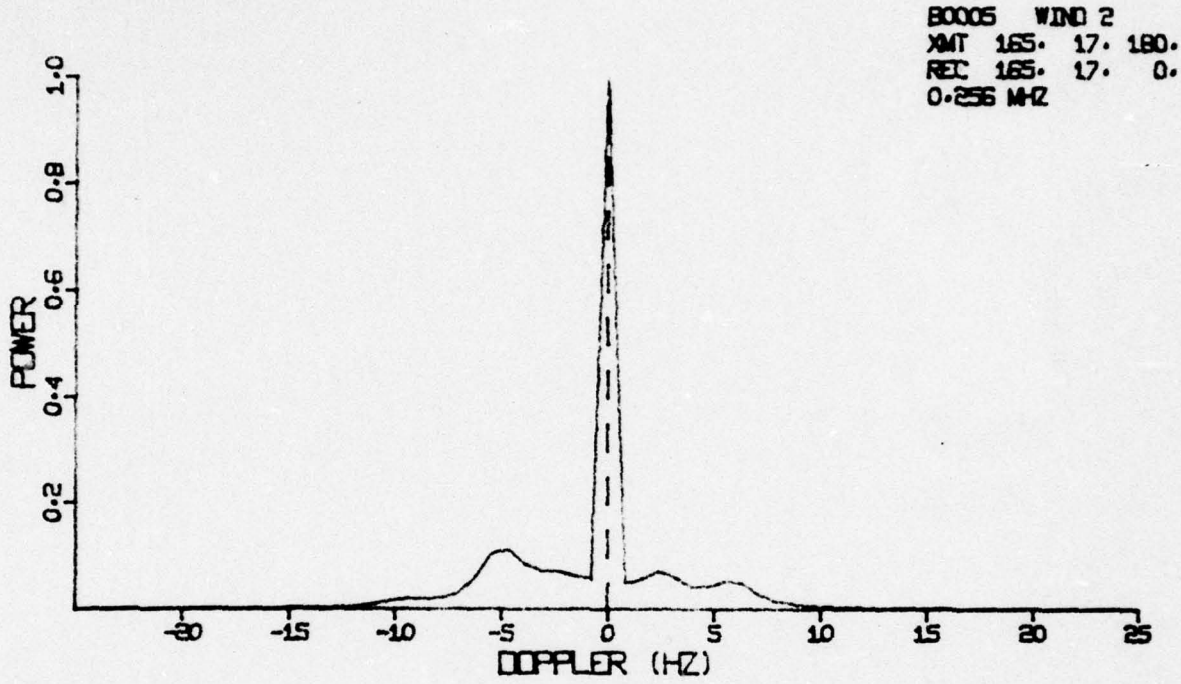


Figure A-1a.

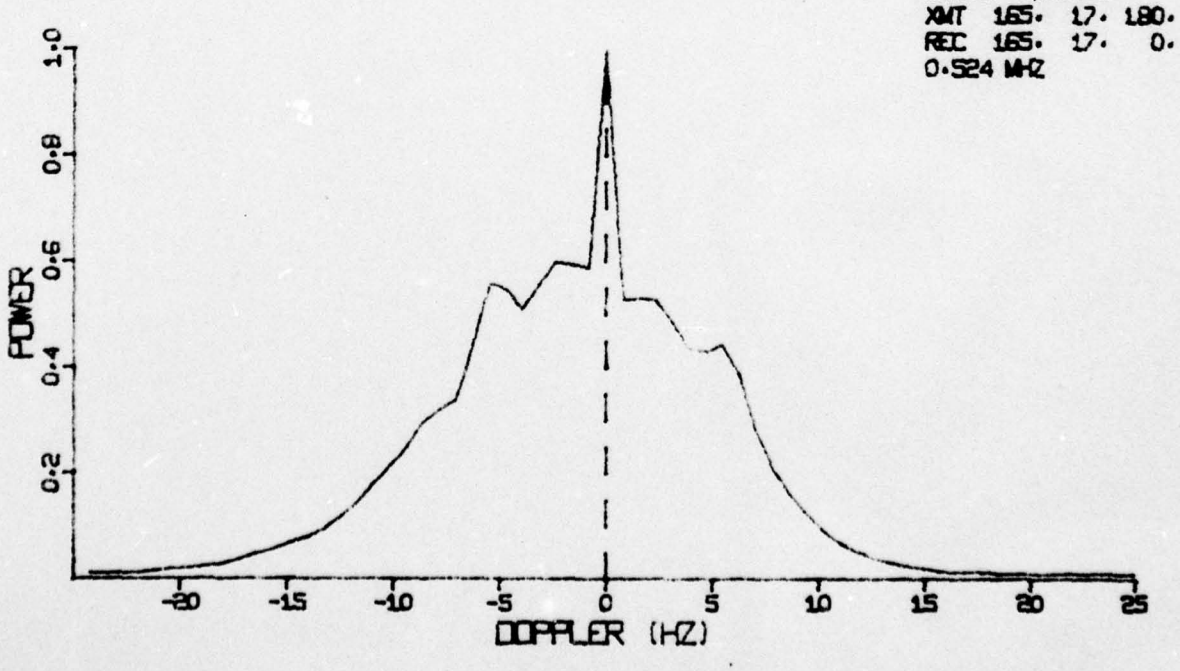


Figure A-1b.

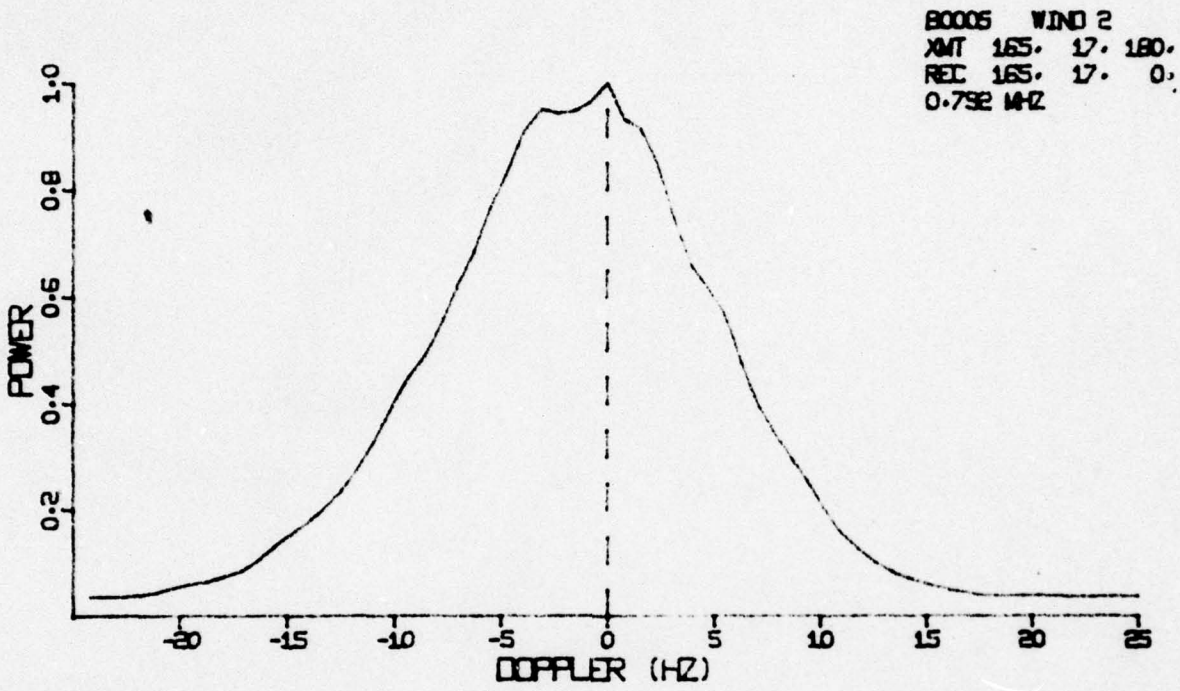


Figure A-1c.

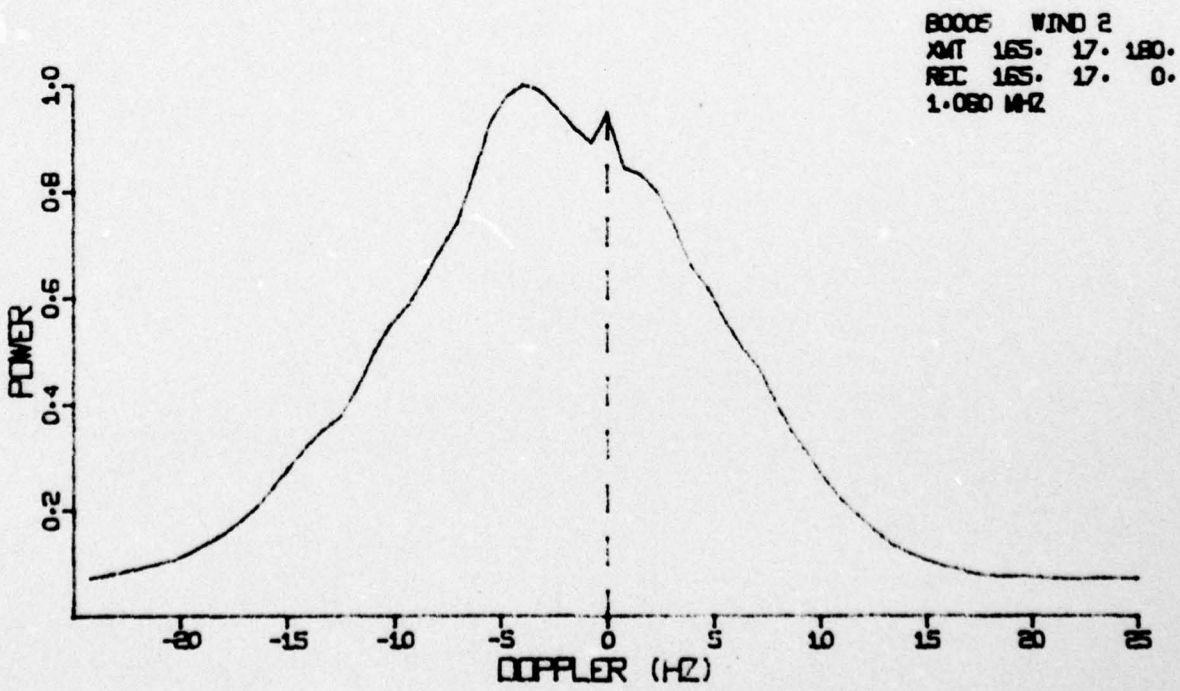


Figure A-1d.

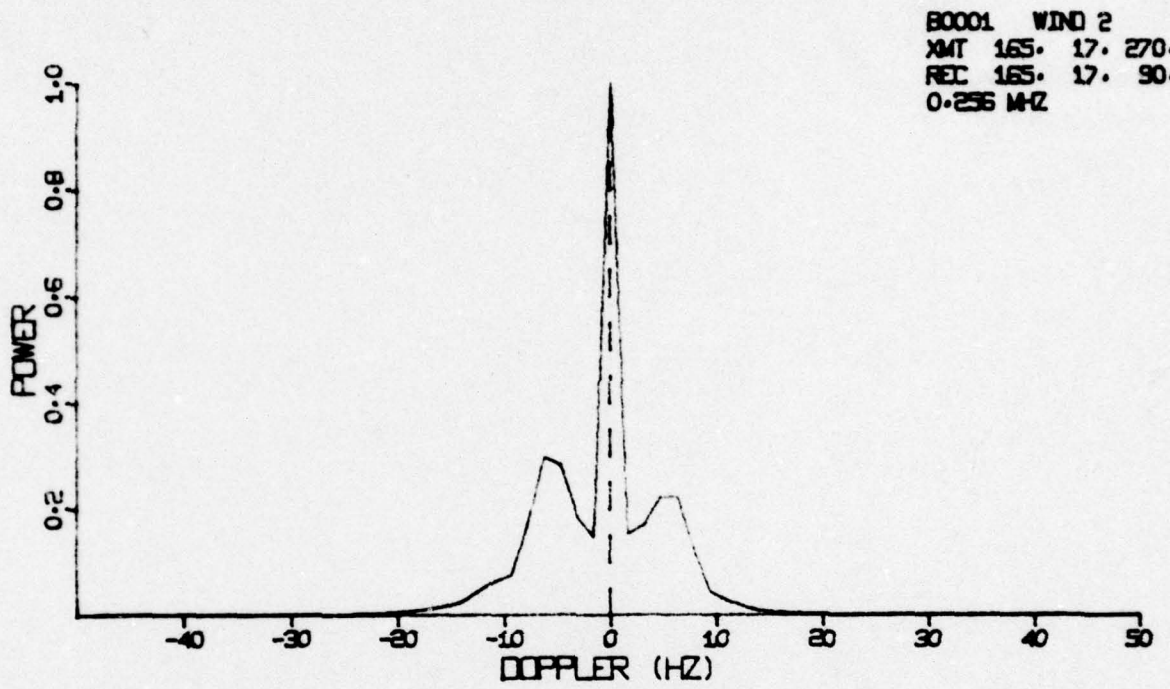


Figure A-2a.

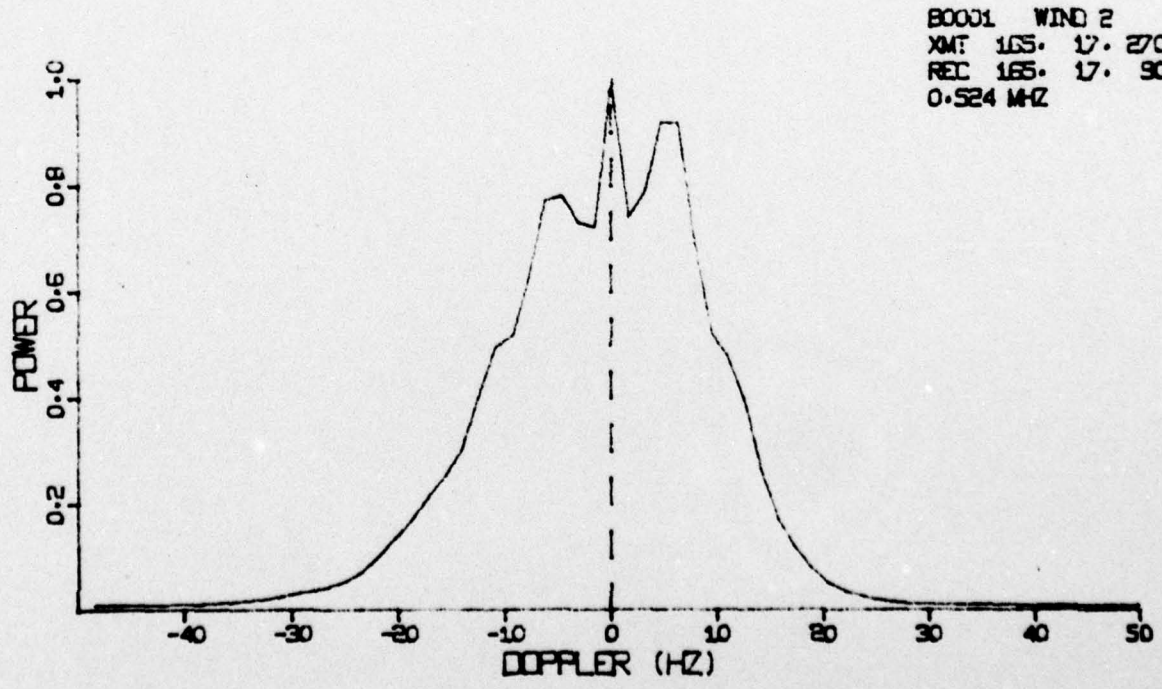


Figure A-2b.

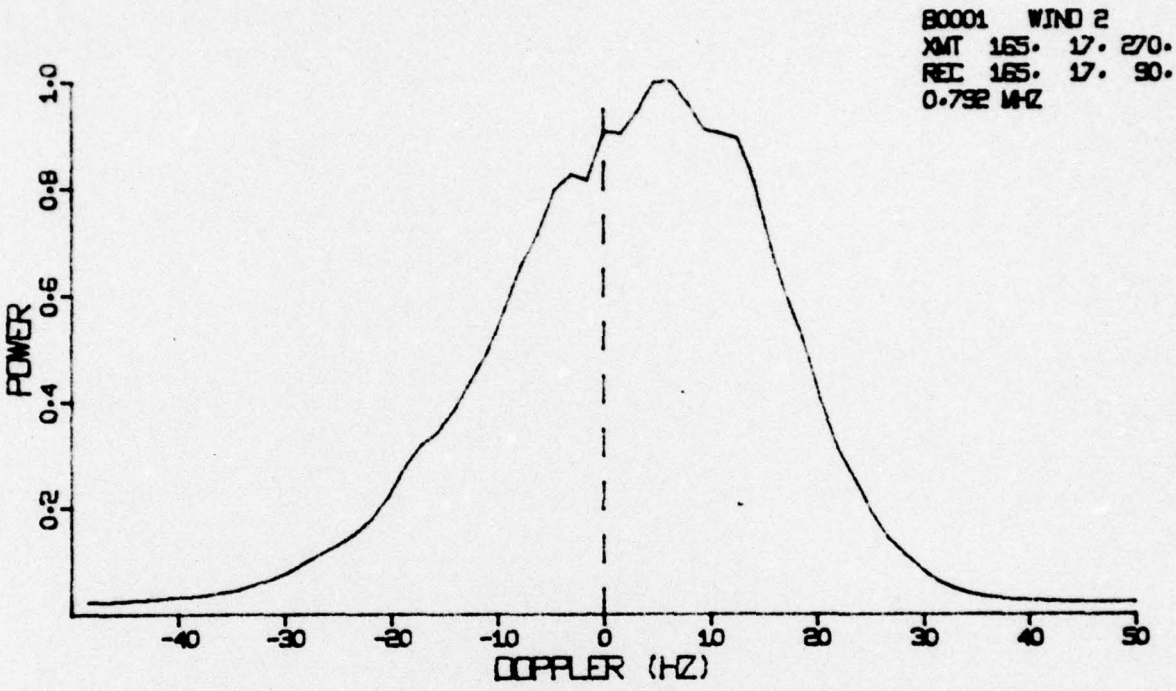


Figure A-2c.

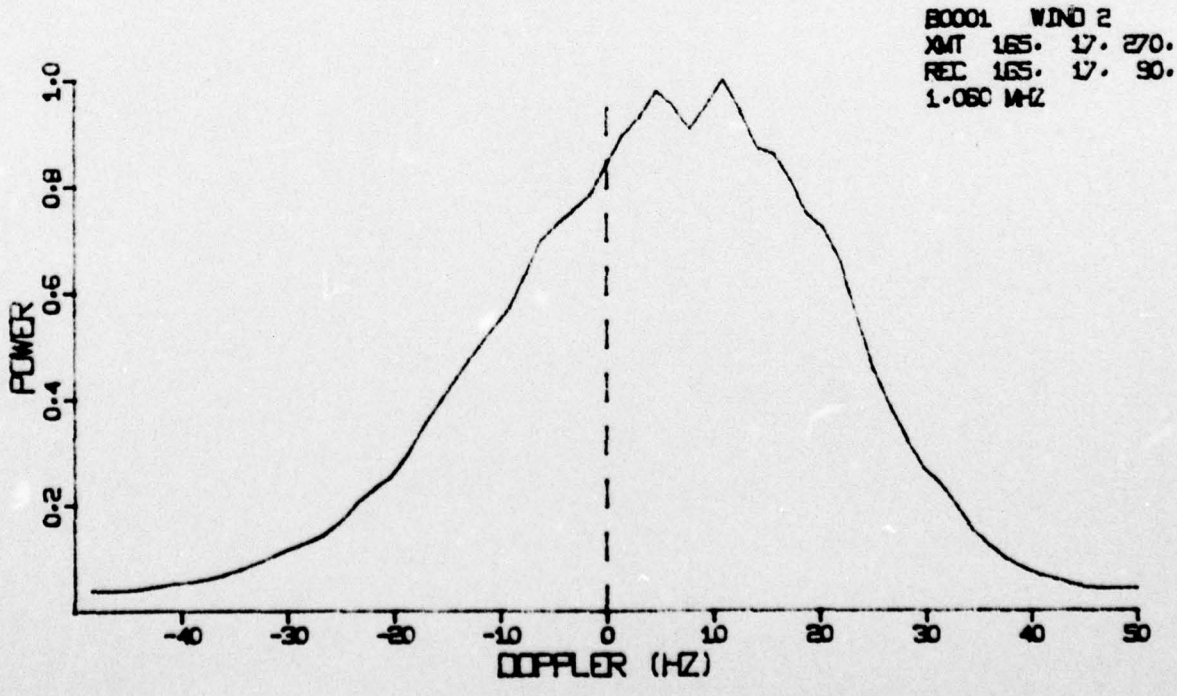


Figure A-2d.

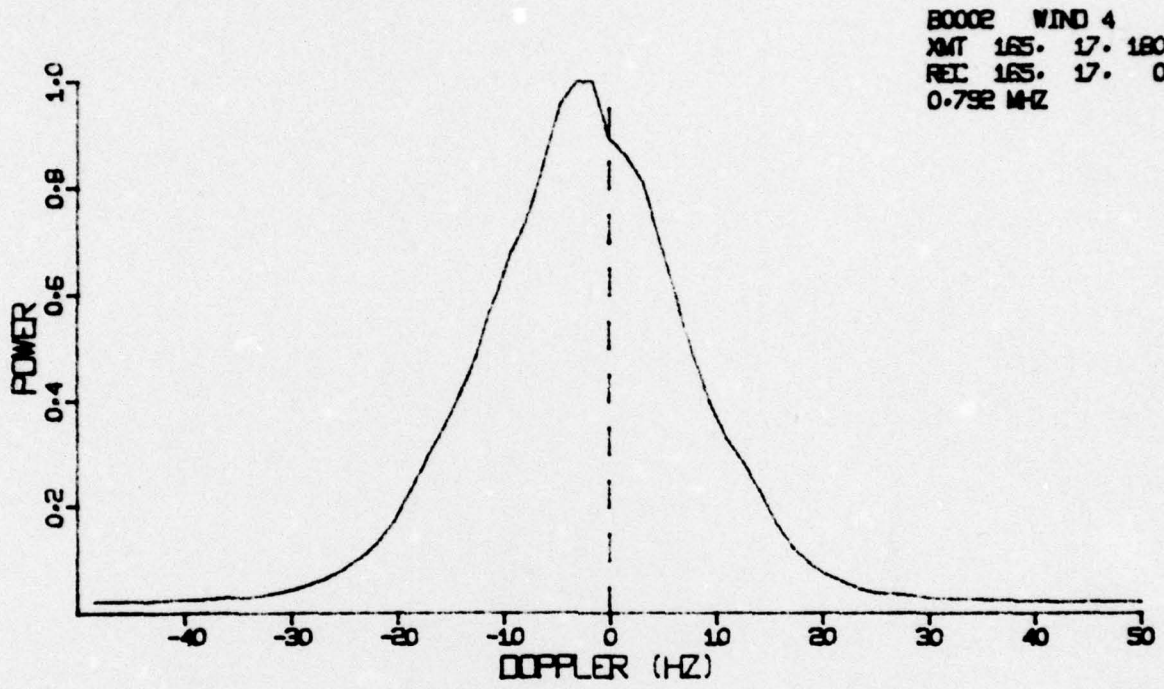


Figure A-3c.

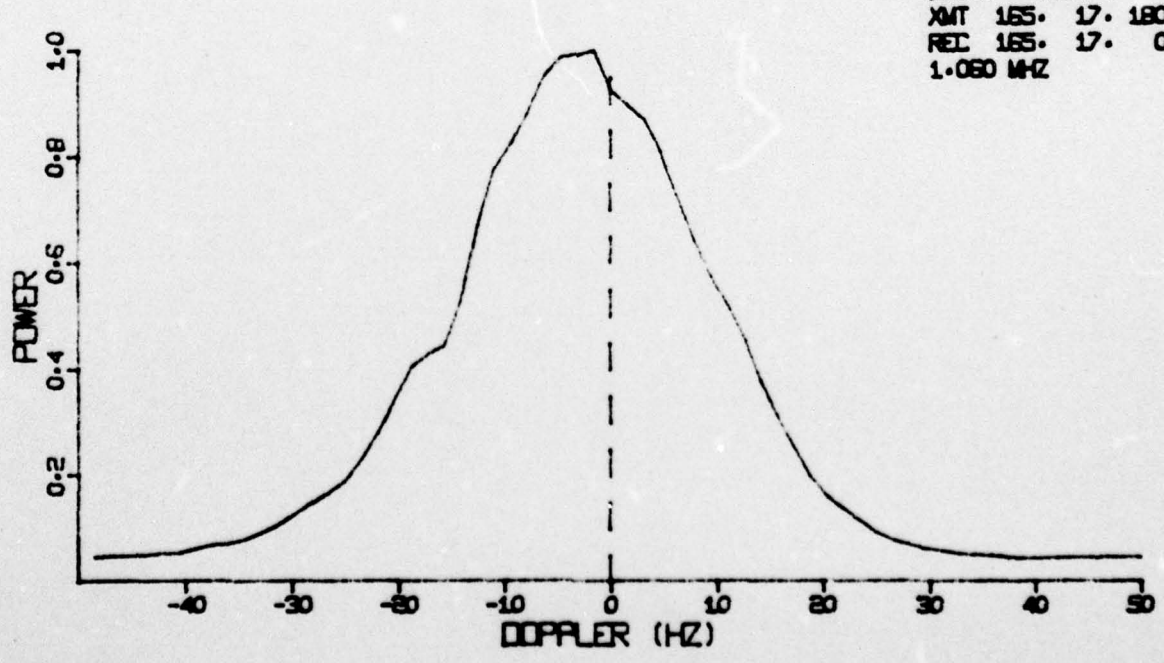


Figure A-3d.

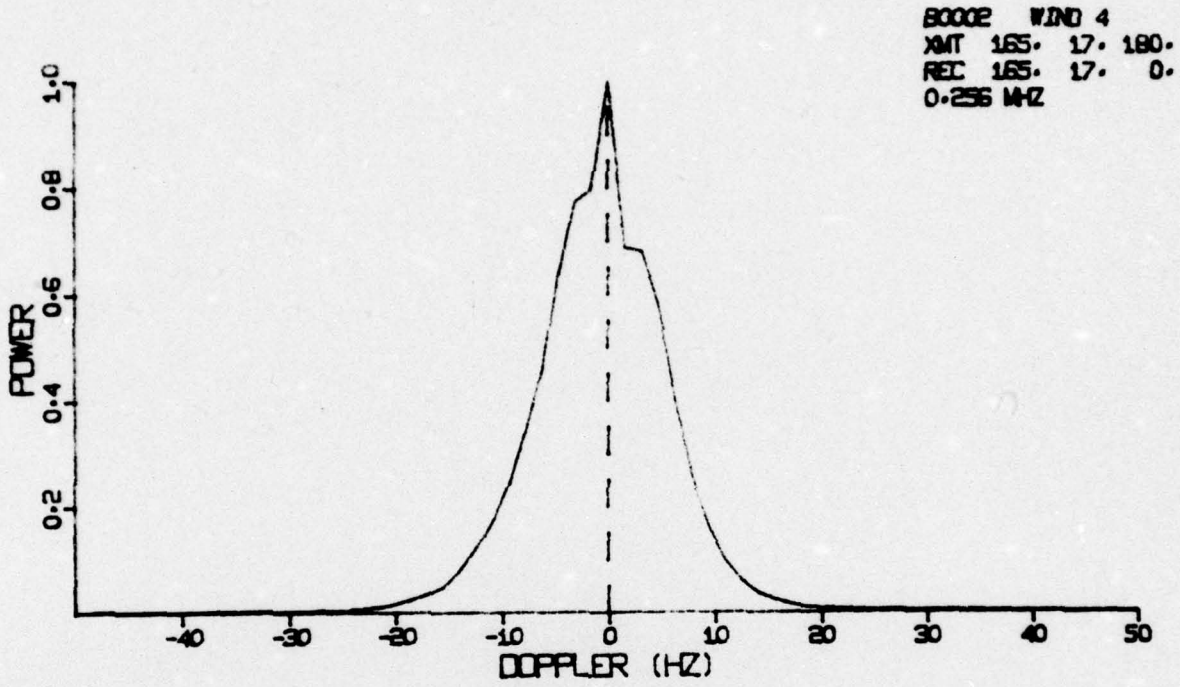


Figure A-3a.

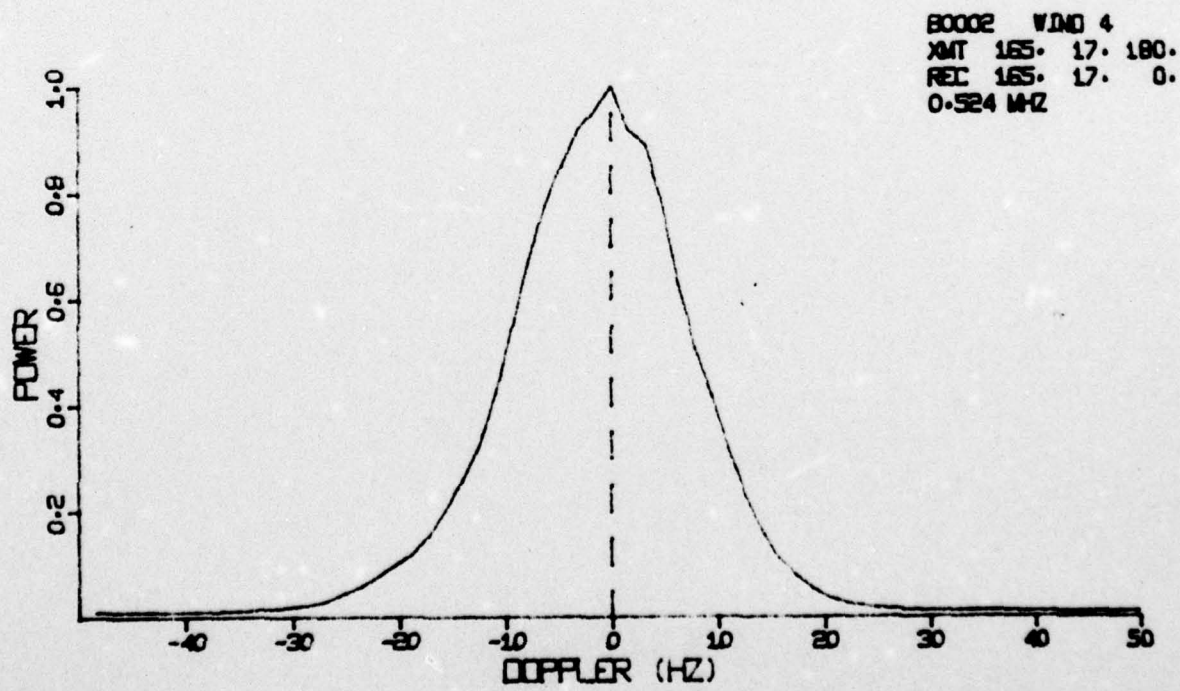


Figure A-3b.

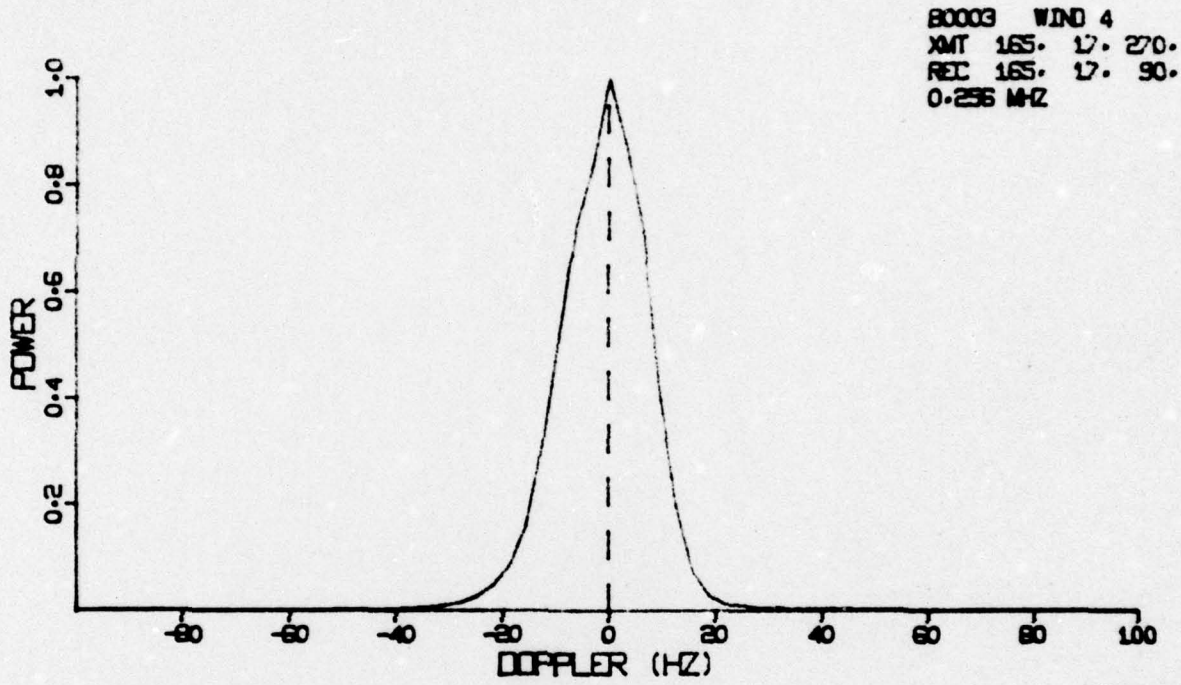


Figure A-4a.

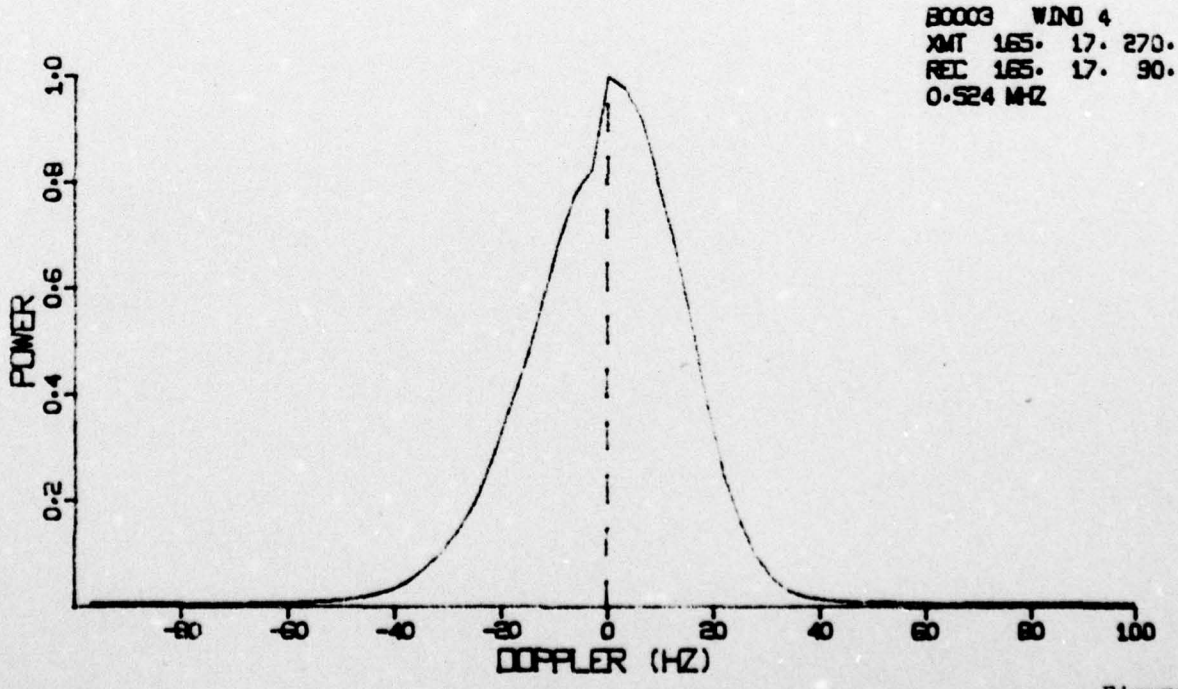


Figure A-4b.

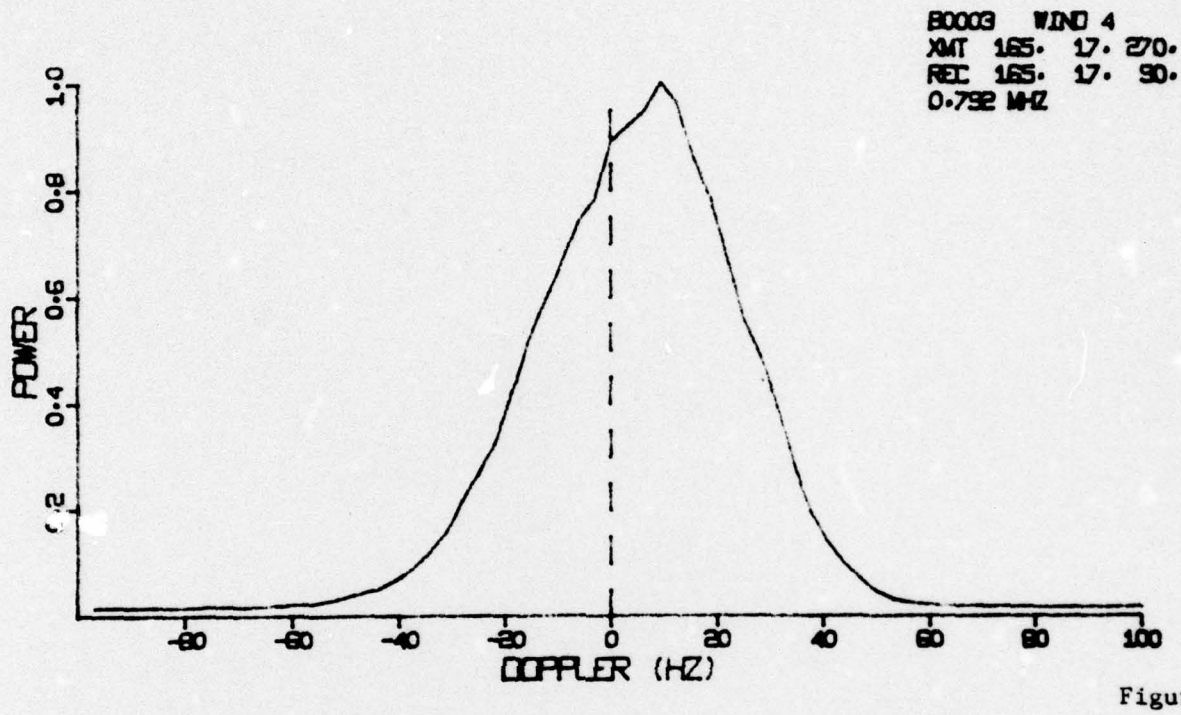


Figure A-4c.

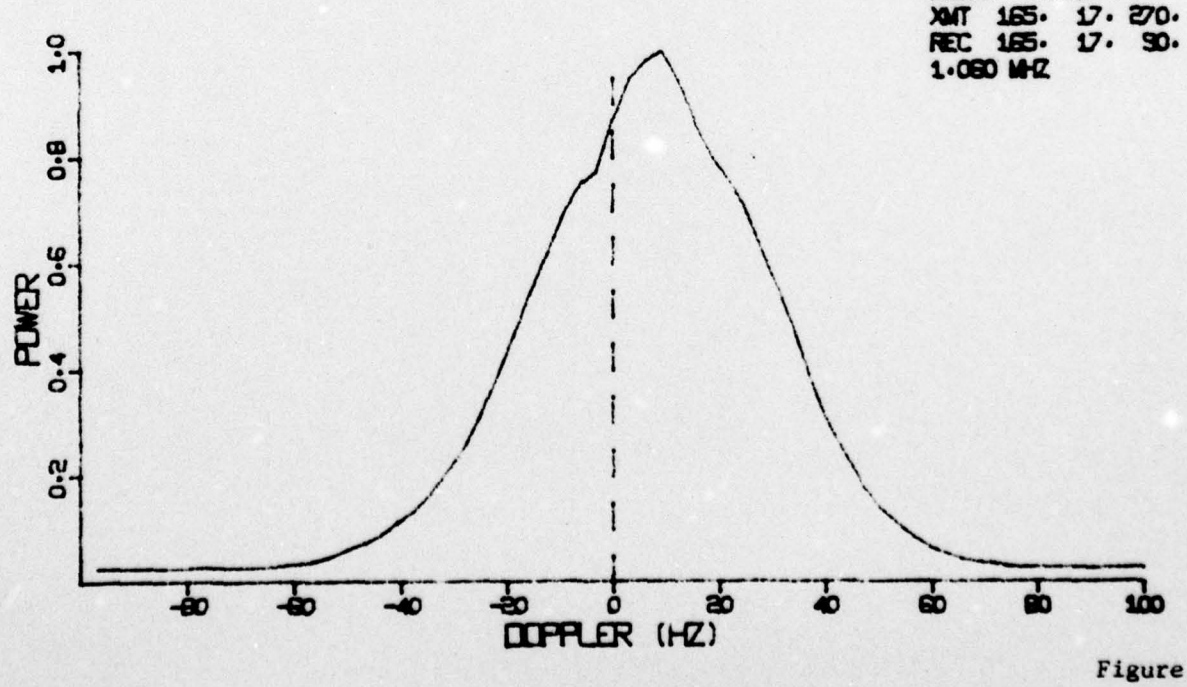


Figure A-4d.

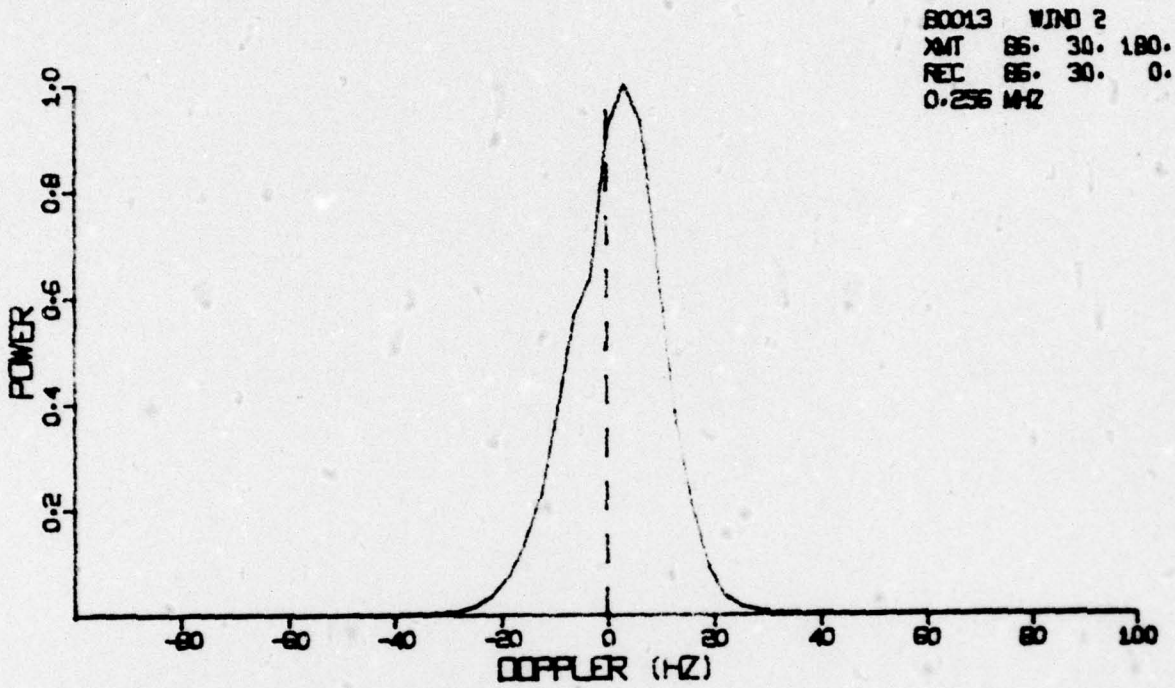


Figure A-5a.

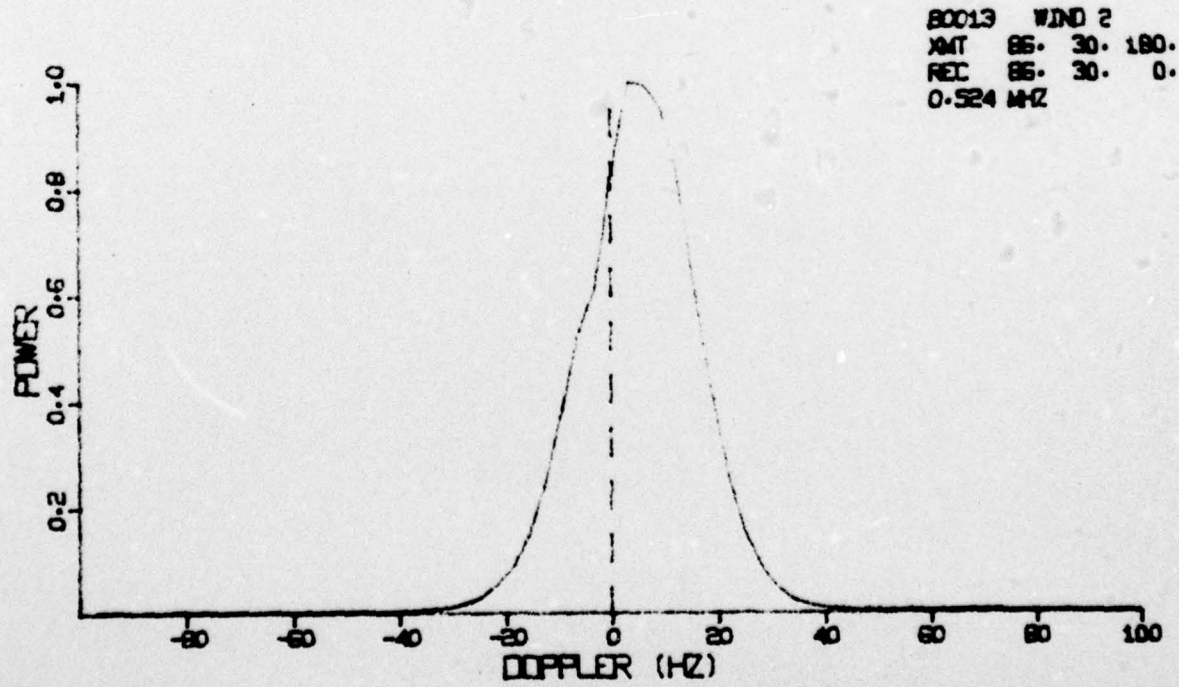


Figure A-5b.

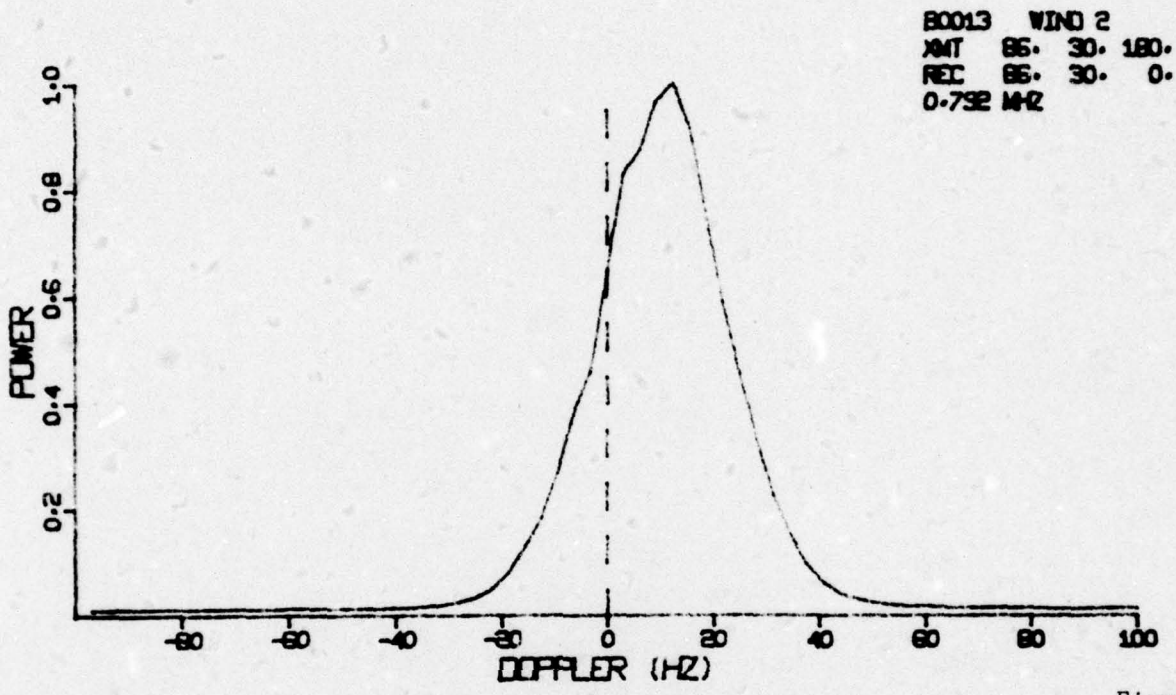


Figure A-5c.

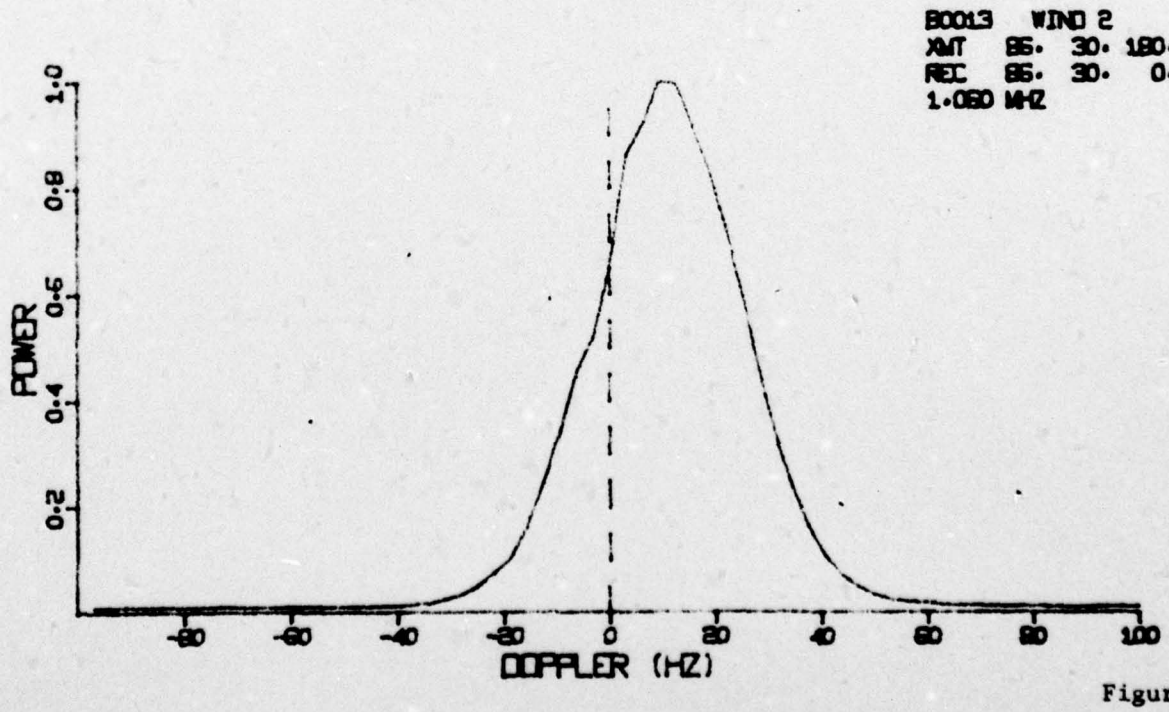


Figure A-5d.

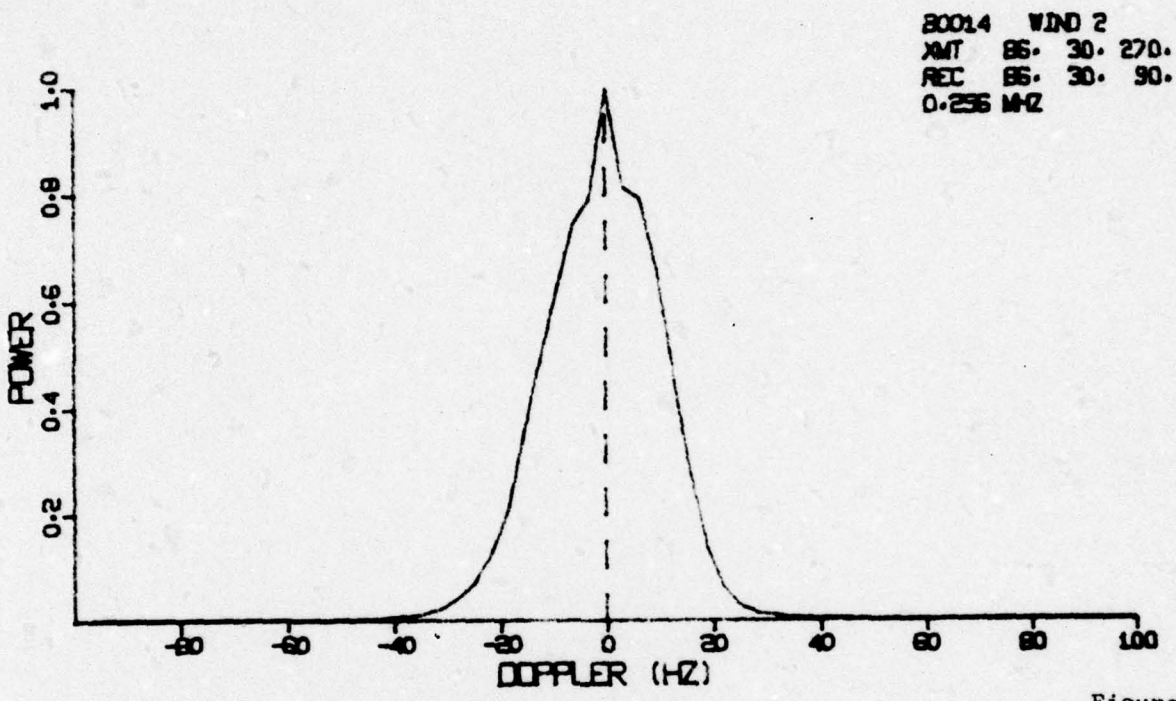


Figure A-6a.

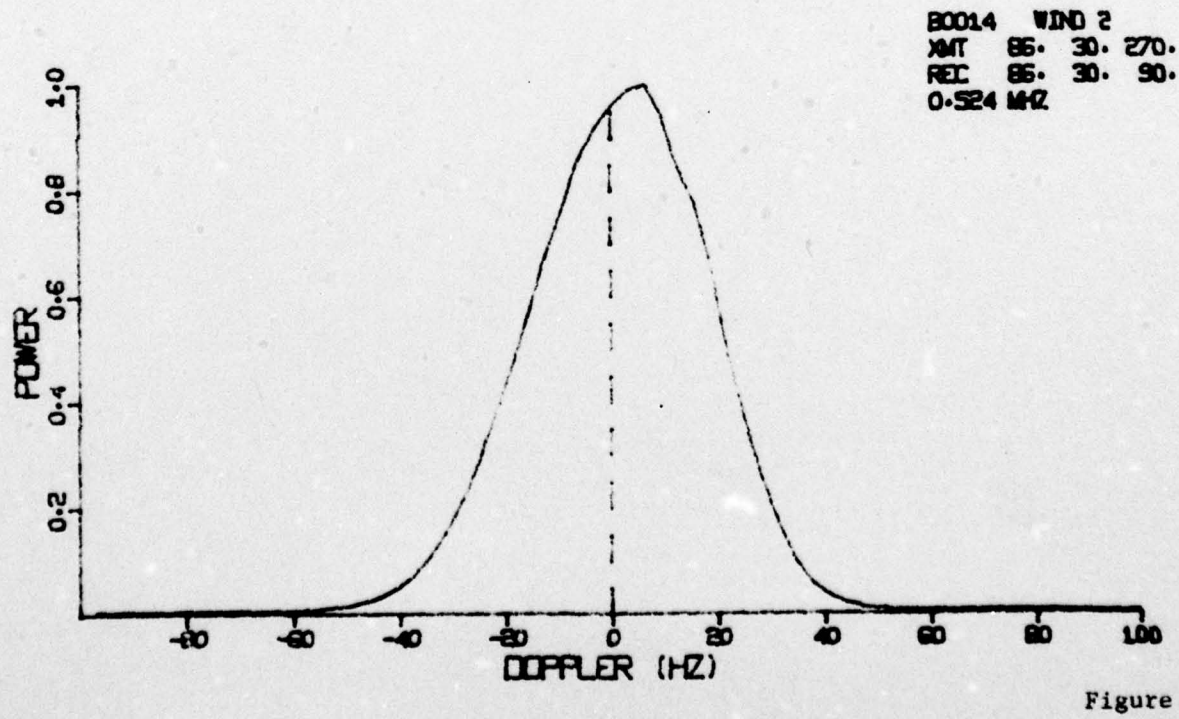


Figure A-6b.

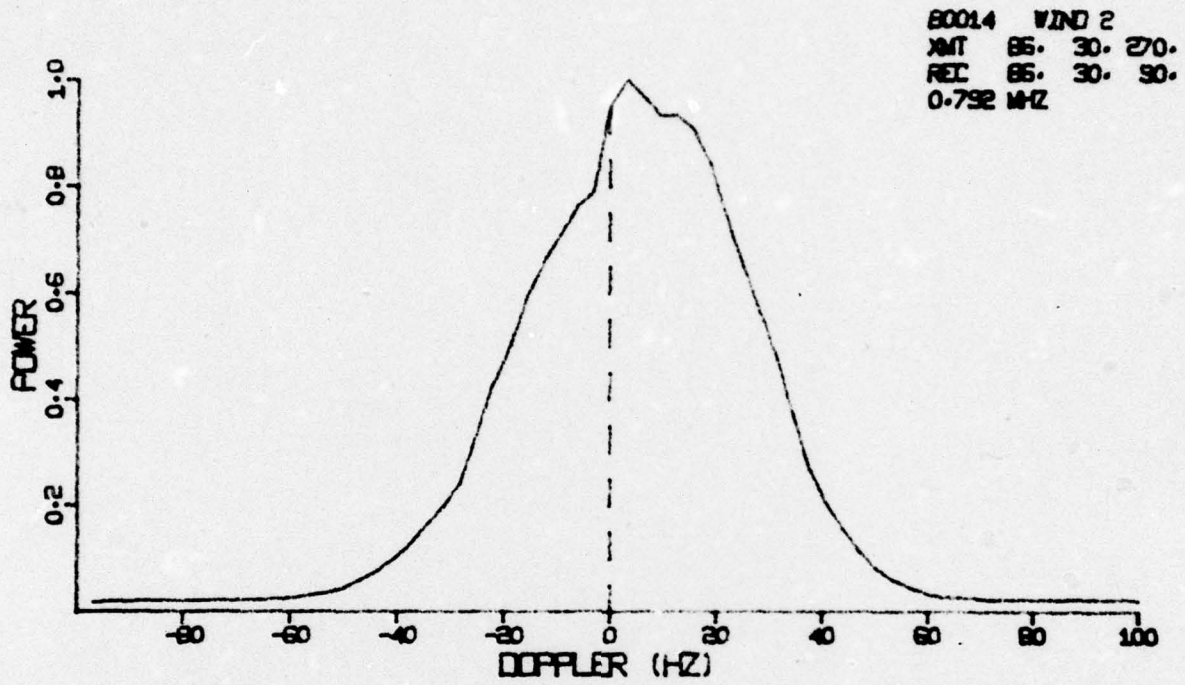


Figure A-6c.

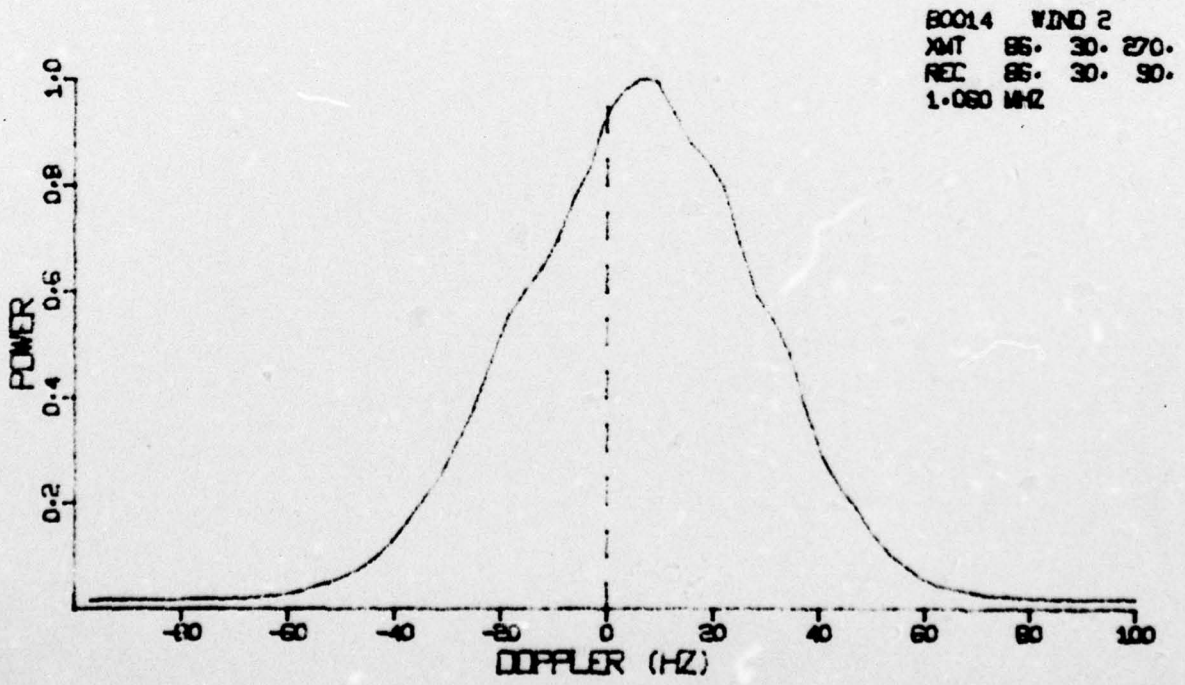


Figure A-6d.

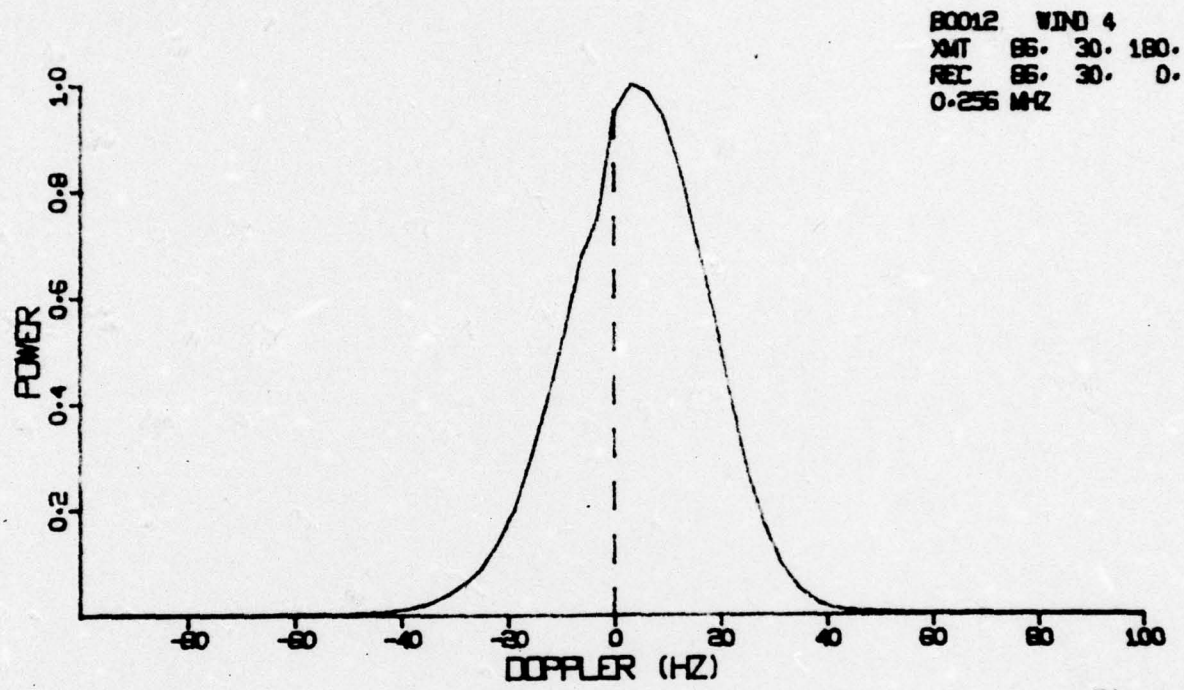


Figure A-7a.

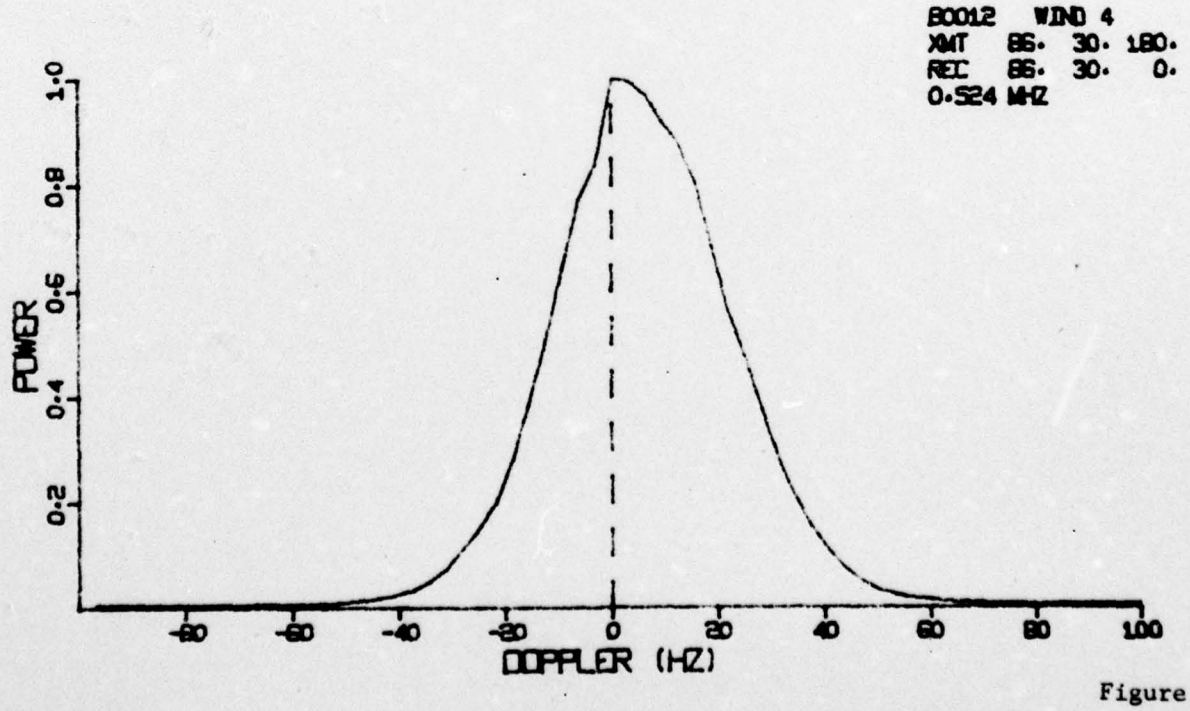


Figure A-7b.

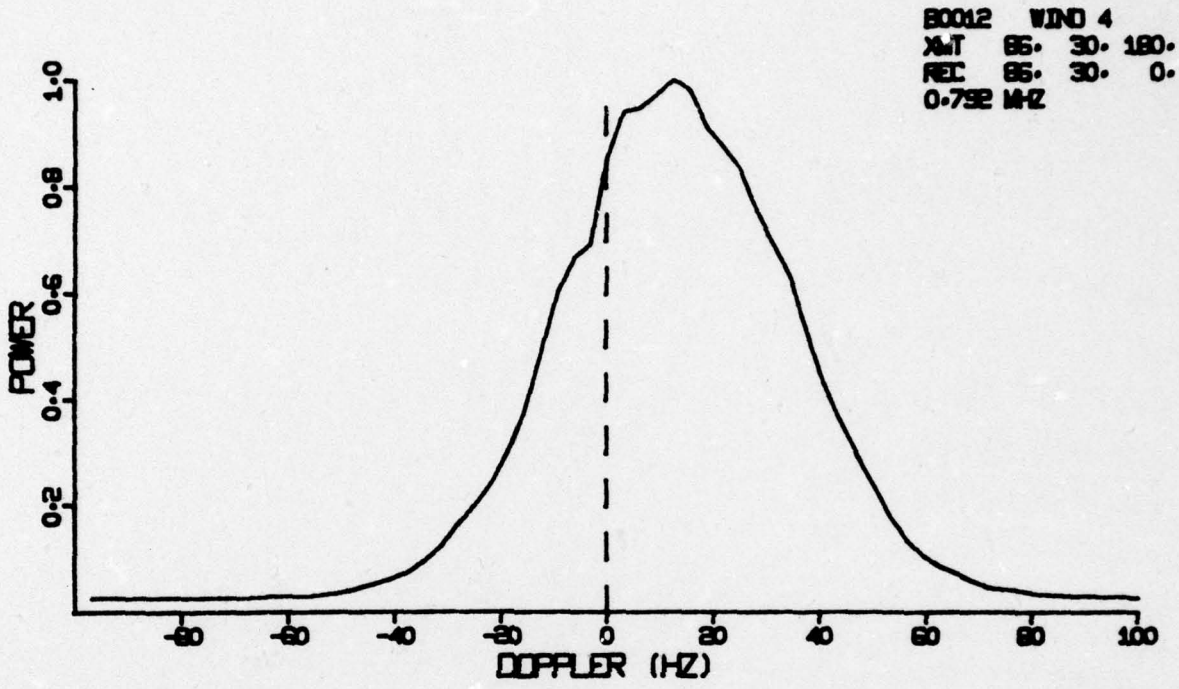


Figure A-7c.

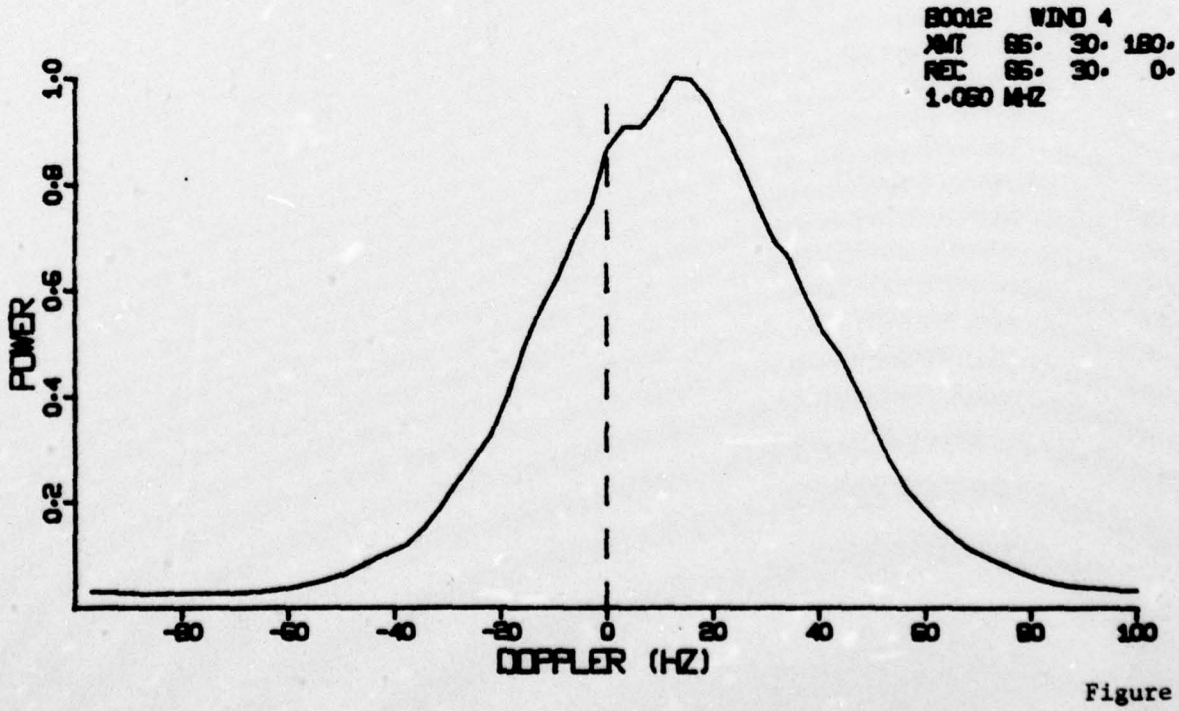


Figure A-7d.

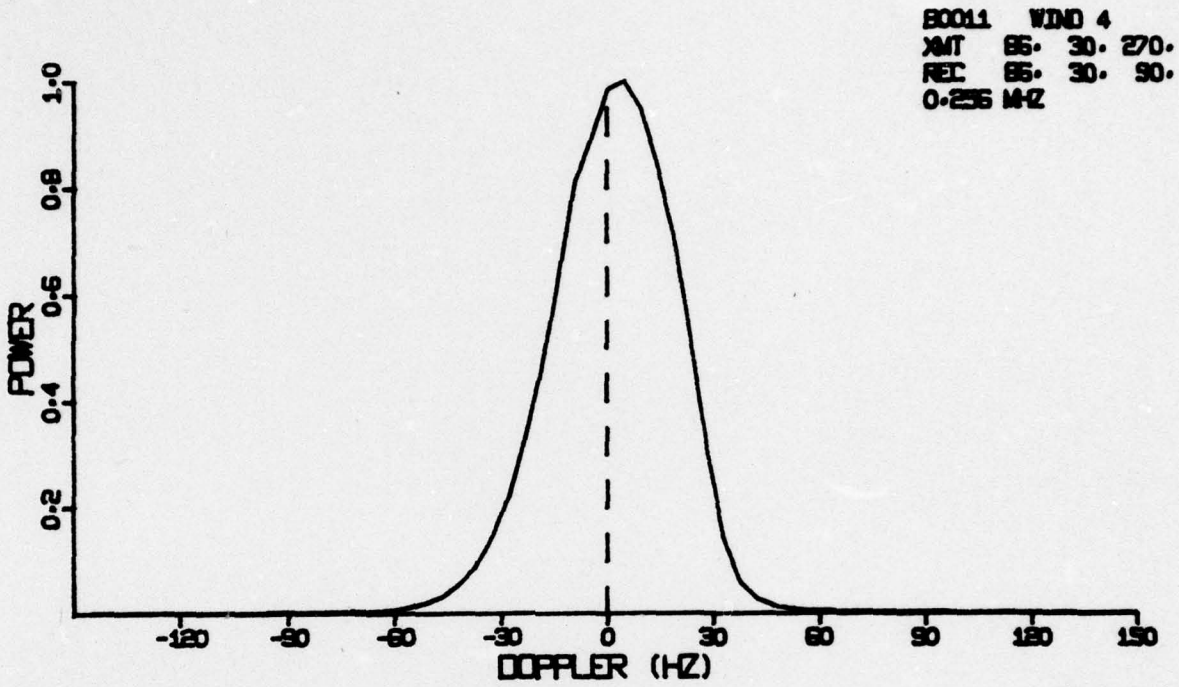


Figure A-8a.

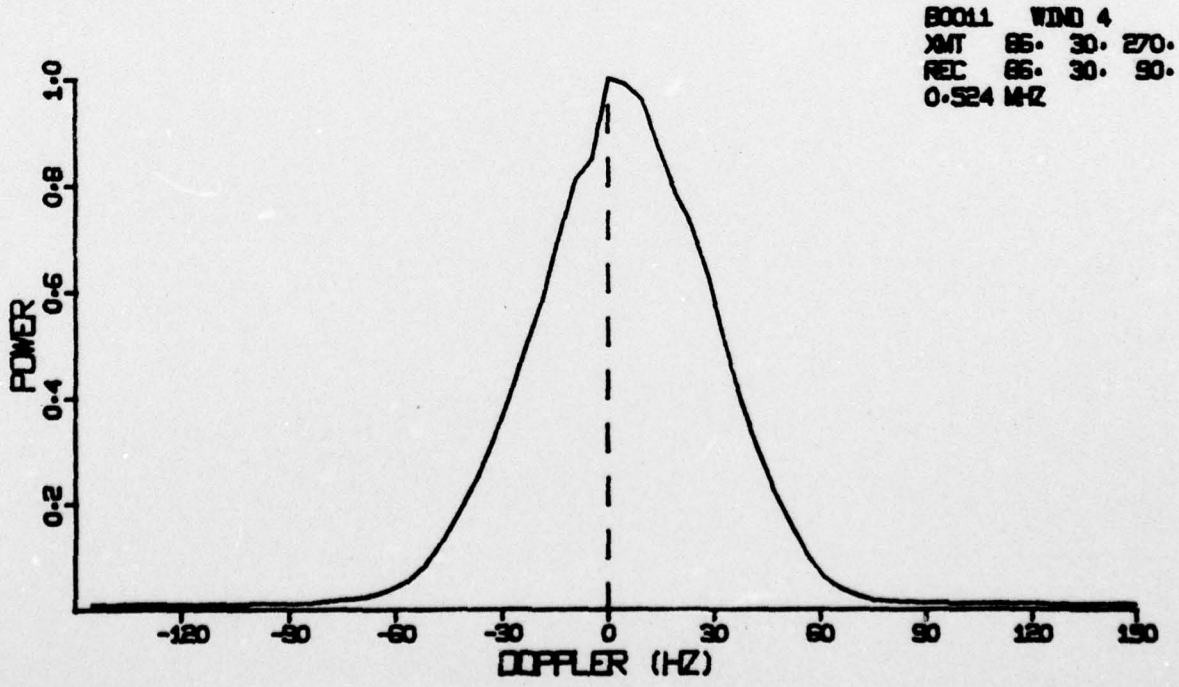


Figure A-8b.

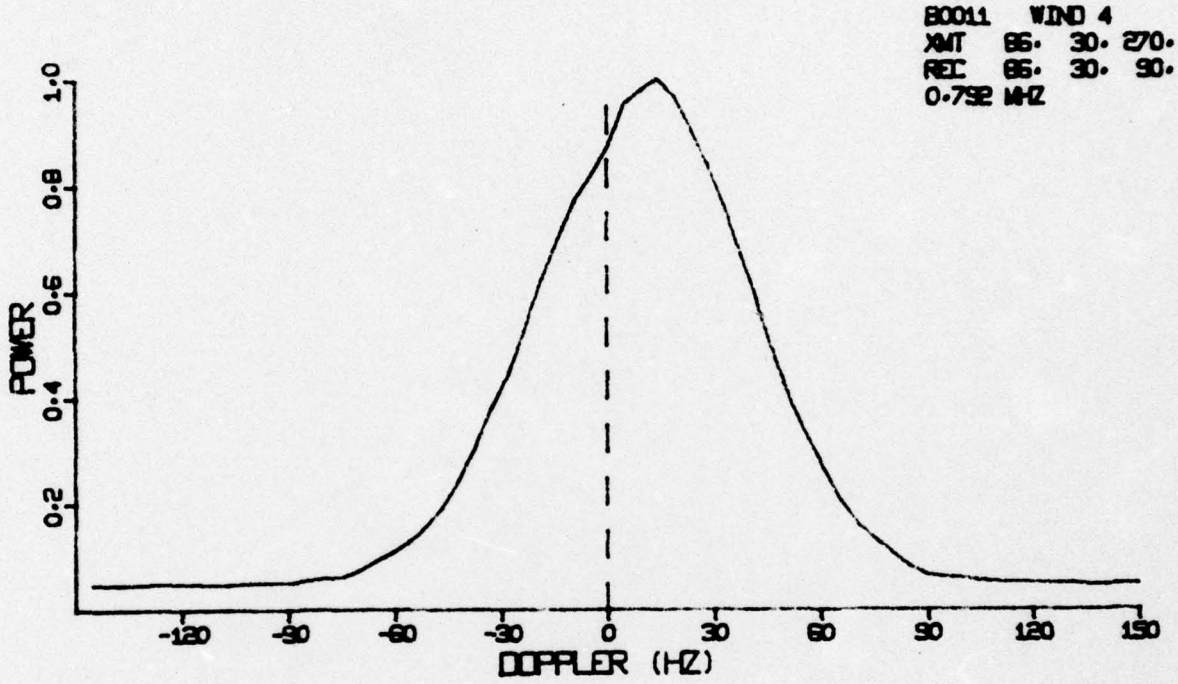


Figure A-8c.

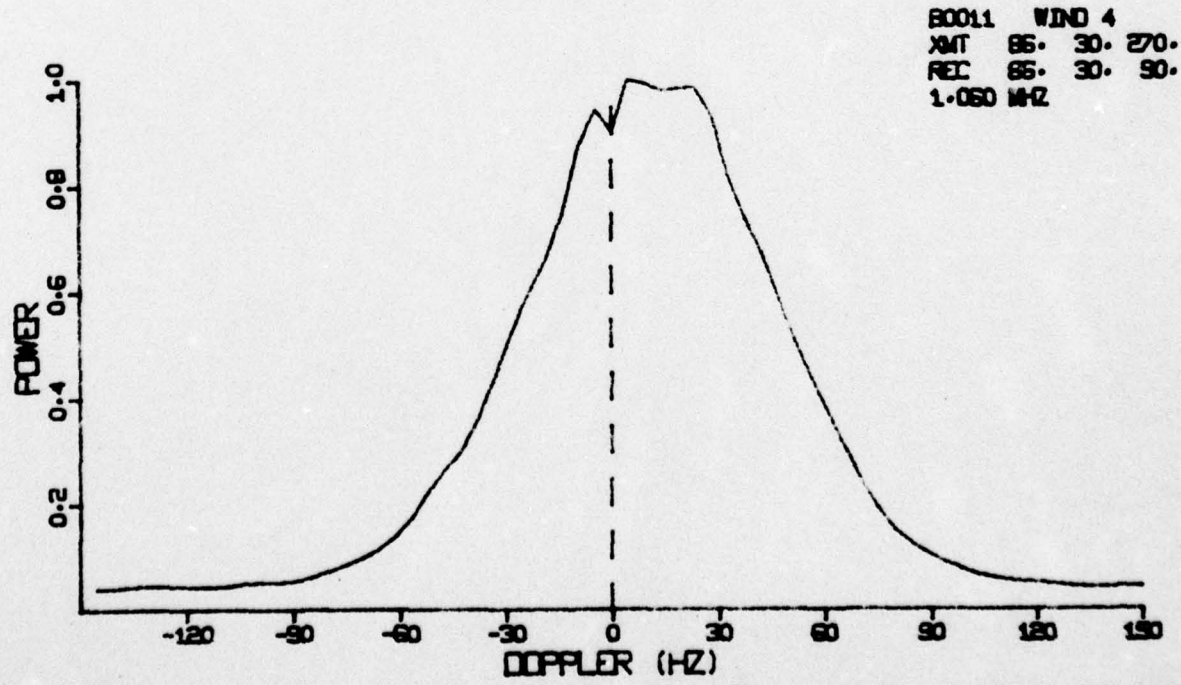


Figure A-8d.